

DOT/FAA/TC-20/12

Federal Aviation Administration
William J. Hughes Technical Center
Aviation Research Division
Atlantic City International Airport
New Jersey 08405

Thermal Runaway Initiation Methods for Lithium Batteries

July 2019

Final Report

This document is available to the U.S. public through the National Technical Information Services (NTIS), Springfield, Virginia 22161.

This document is also available from the Federal Aviation Administration William J. Hughes Technical Center at actlibrary.tc.faa.gov.



U.S. Department of Transportation
Federal Aviation Administration

NOTICE

This document is disseminated under the sponsorship of the U.S. Department of Transportation in the interest of information exchange. The U.S. Government assumes no liability for the contents or use thereof. The U.S. Government does not endorse products or manufacturers. Trade or manufacturers' names appear herein solely because they are considered essential to the objective of this report. The findings and conclusions in this report are those of the author(s) and do not necessarily represent the views of the funding agency. This document does not constitute FAA policy. Consult the FAA sponsoring organization listed on the Technical Documentation page as to its use.

This report is available at the Federal Aviation Administration William J. Hughes Technical Center's Full-Text Technical Reports page: actlibrary.tc.faa.gov in Adobe Acrobat portable document format (PDF).

Technical Report Documentation Page

1. Report No. DOT/FAA/TC-20/12		2. Government Accession No.		3. Recipient's Catalog No.	
4. Title and Subtitle Thermal Runaway Initiation Methods for Lithium Batteries				5. Report Date July 2019	
				6. Performing Organization Code ANG-E21	
7. Author(s) Matthew Karp				8. Performing Organization Report No.	
9. Performing Organization Name and Address U.S. Department of Transportation William J. Hughes Technical Center Aviation Research Division Fire Safety Branch, ANG-E21 Atlantic City International Airport, NJ 0840				10. Work Unit No. (TRAIS)	
				11. Contract or Grant No. NA	
12. Sponsoring Agency Name and Address FAA Northwest Mountain Regional Office 1601 Lind Avenue SW Renton, WA 98057				13. Type of Report and Period Covered Final Report	
				14. Sponsoring Agency Code AXH-001	
15. Supplementary Notes					
16. Abstract <p>The prevalence of lithium batteries on aircraft is a potential safety hazard because of the risk of thermal runaway—a rapid rise in temperature and pressure, and the release of flammable gases. The goal of this study was to create a framework for potential guidelines for a standardized test method for the classification of a lithium battery’s cell hazard due to thermal runaway. Classifying a cell’s hazards due to thermal runaway can help determine appropriate mitigation methods for their use and transport.</p> <p>Some of the cells were overcharged and other cells were overheated at various heating rates to force thermal runaway. The maximum cell case temperature, cell case temperature at the onset of thermal runaway, and peak percent pressure rise were measured. The thermal runaway vent gases were collected and analyzed for hydrogen, carbon monoxide, carbon dioxide, and hydrocarbon concentrations. The gas and pressure measurements were used to calculate the lower flammability limit (LFL) of the vent gas. The average maximum air-filled volumes that become flammable per cell after thermal runaway were determined and evaluated.</p> <p>Lithium manganese dioxide (LiMnO₂) cylindrical primary cells at 100% state of charge (SOC) of type CR123a 3V 1500mAh were tested. There were differences between the overheat method and the overcharge method. The methods varied by test duration, repeatability, and test results. The overheat method was the quickest and most repeatable method for producing a thermal runaway event. Lithium cobalt oxide (LiCoO₂) cylindrical secondary cells at 30% SOC, of type 18650 3.7V 2600mAh were tested at various heating rates. The results suggest that the heating rate significantly affects an 18650-sized cell’s thermal runaway. Cells heated with a heating rate of less than 12°C/min produced a lesser quantity of vent gas and measured a lower maximum cell case temperature than cells heated with a heating rate of more than 17°C/min. A heating rate between 12°C/min and 17°C/min produced mixed results. LiCoO₂ pouch cells at 30% SOC 3.7V 2500mAh, were also tested at various heating rates. The results suggest that the heating rate moderately affects a pouch cell’s thermal runaway. For every 10 C°/min increase in heating rate, the total vent-gas volume increased by 0.057 L, the percent pressure rise increased by 0.89%, and the concentration of carbon dioxide decreased by 2.3%.</p>					
17. Key Words lithium, lithium-ion, battery, batteries, cells, thermal runaway, gas analysis			18. Distribution Statement This document is available to the U.S. public through the National Technical Information Service (NTIS), Springfield, Virginia 22161. This document is also available from the Federal Aviation Administration William J. Hughes Technical Center at actlibrary.tc.faa.gov .		
19. Security Classif. (of this report) Unclassified		20. Security Classif. (of this page) Unclassified		21. No. of Pages 48	22. Price

TABLE OF CONTENTS

EXECUTIVE SUMMARY	IX
1. INTRODUCTION	1
1.1 BACKGROUND	1
1.2 OBJECTIVE	1
2. GENERAL TEST PROCEDURE	2
2.1 LE CHATELIER'S MIXING RULE	4
2.2 MAXIMUM FLAMMABLE AIR-FILLED VOLUME PER CELL	5
2.3 STATISTICAL ANALYSIS	5
2.3.1 OVERHEAT AND OVERCHARGE METHOD COMPARISON	5
2.4 HEATING RATE COMPARISON TEST PROCEDURE	8
3. DISCUSSION OF RESULTS – OVERHEAT AND OVERCHARGE METHOD COMPARISON – CR123A CELL	12
3.1 INITIATION METHODS POST TEST VISUAL EXAMINATION – CR123A CELL	12
3.2 VOLTAGE DURING OVERHEAT – CR123A CELL	15
3.3 METHODS AND THERMAL RUNAWAY ONSET TEMPERATURE – CR123A CELL	16
3.4 METHODS AND MAXIMUM CELL CASE TEMPERATURE – CR123A CELL	17
3.5 METHODS AND VENT GAS VOLUME – CR123A CELL	18
3.6 METHODS AND PERCENT PRESSURE RISE – CR123A CELL	19
3.7 METHODS AND TOTAL HYDROCARBON CONTENT – CR123A CELL	20
4. DISCUSSION OF RESULTS - HEATING RATE COMPARISON – 18650 CELL	21
4.1 HEATING RATE AND THERMAL RUNAWAY ONSET TEMPERATURE – 18650 CELL	21
4.2 HEATING RATE AND MAXIMUM CELL CASE TEMPERATURE – 18650 CELL	22

4.3 HEATING RATE AND VENT GAS VOLUME – 18650 CELL	23
4.4 HEATING RATE AND REACTION TYPE – 18650 CELL	24
4.5 REACTION TYPE AND MAXIMUM CELL CASE TEMPERATURE – 18650 CELL	26
4.6 REACTION TYPE AND VENT GAS VOLUME – 18650 CELL	27
4.7 REACTION TYPE AND PERCENT PRESSURE RISE – 18650 CELL	28
4.8 REACTION TYPE AND HYDROGEN CONCENTRATION – 18650 CELL	29
4.9 REACTION TYPE AND TOTAL HYDROGEN VOLUME – 18650 CELL	30
4.10 REACTION TYPE AND CARBON DIOXIDE CONCENTRATION – 18650 CELL	31
4.11 REACTION TYPE AND TOTAL CARBON DIOXIDE VOLUME – 18650 CELL	32
4.12 LE CHATELIER’S MIXING RULE CALCULATION – 18650 CELL	33
5. DISCUSSION OF RESULTS – HEATING RATE COMPARISON – POUCH CELL	34
5.1 HEATING RATE AND MAXIMUM CELL CASE TEMPERATURE – POUCH CELL	34
5.2 HEATING RATE AND VENT GAS VOLUME – POUCH CELL	35
5.3 HEATING RATE AND PERCENT PRESSURE RISE – POUCH CELL	36
5.4 HEATING RATE AND HYDROGEN CONCENTRATION – POUCH CELL	37
5.5 HEATING RATE AND TOTAL HYDROGEN VOLUME – POUCH CELL	37
5.6 HEATING RATE AND CARBON DIOXIDE CONCENTRATION – POUCH CELL	37
5.7 HEATING RATE AND TOTAL CARBON DIOXIDE VOLUME – POUCH CELL	38
5.8 LE CHATELIER’S MIXING RULE CALCULATION – POUCH CELL	38
6. SUMMARY OF RESULTS	39
7. REFERENCES	42

LIST OF FIGURES

Figure 1. Test apparatus: 21.7 L pressure vessel used for testing	2
Figure 2. Overheat with battery holder assembly – CR123a cell	7
Figure 3. Overheat without battery holder assembly – CR123a cell	7
Figure 4. Overcharge with modified battery holder assembly – CR123a cell	8
Figure 5. Overheat setup – 18650 cell	9
Figure 6. Cell thermocouple location – pouch cell	10
Figure 7. Cell case temperature versus time by thermocouple location at 10°C/min – pouch cell	10
Figure 8. Cell case temperature versus time by heating rate – 18650 cell	11
Figure 9. Cell case temperature versus time by heating rate – pouch cell	12
Figure 10. Thermal runaway by overheating with battery holder assembly – CR123a cell	13
Figure 11. Thermal runaway by overheating without battery holder assembly – CR123a cell	13
Figure 12. Deformation of cell casing due to thermal runaway by overcharging – CR123a cell	14
Figure 13. Deformation of cell casing due to energetic failure by overcharging – CR123a cell	15
Figure 14. Cell case temperature and voltage output versus time - CR123a cell	16
Figure 15. Thermal runaway onset temperature versus method – CR123a cell	17
Figure 16. Maximum cell case temperature versus method – CR123a cell	18
Figure 17. Vent gas volume versus method – CR123a cell	19
Figure 18. Percent pressure rise versus method – CR123a cell	20
Figure 19. Total hydrocarbon content versus method– CR123a cell	21
Figure 20. Thermal runaway onset temperature versus heating rate – 18650 cell	22
Figure 21. Maximum cell case temperature versus heating rate – 18650 cell	23

Figure 22. Vent gas volume versus heating rate – 18650 cell	24
Figure 23. Maximum cell case temperature and vent gas volume versus heating rate – 18650 cell	25
Figure 24. Reaction type versus heating rate – 18650 cell	26
Figure 25. Maximum cell case temperature versus reaction type – 18650 cell	27
Figure 26. Cell vent gas volume versus reaction type – 18650 cell	28
Figure 27. Percent pressure rise versus reaction type – 18650 cell	29
Figure 28. Hydrogen concentration versus reaction type – 18650 cell	30
Figure 29. Total volume of hydrogen versus reaction type – 18650 cell	31
Figure 30. Concentration of carbon dioxide versus reaction type – 18650 cell	32
Figure 31. Carbon dioxide volume versus reaction type – 18650 cell	33
Figure 32. Maximum cell case temperature versus heating rate – pouch cell	35
Figure 33. Total vent gas volume versus heating rate – pouch cell	36
Figure 34. Percent pressure rise versus heating rate – pouch cell	37
Figure 35. CO ₂ concentration vs heating rate – pouch cell	38

LIST OF TABLES

Table 1. Maximum cell case temperature and reaction type – 18650 cell	26
Table 2. Thermal runaway vent gas volume and reaction type – 18650 cell	27
Table 3. Percent pressure rise and reaction type – 18650 cell	28
Table 4. Hydrogen concentration and reaction type – 18650 cell	29
Table 5. Hydrogen volume and reaction type – 18650 cell	30
Table 6. Carbon dioxide concentration and reaction type – 18650 cell	31
Table 7. Carbon dioxide total volume and reaction type – 18650 cell	32
Table 8. Gas concentration and LFL – 18650 cell	33
Table 9. Gas concentration and LFL – Pouch cell	38
Table 10. Significant parameters of various lithium batteries	42

LIST OF ACRONYMS

SOC	State of charge
DC	Direct current
Ah	Ampere-hour
Wh	Watt-hour
LFL	Lower flammability limit
PTC	Positive temperature coefficient
PID	Proportional-integral-derivative
THC	Total hydrocarbon content
ANOVA	analysis of variance

EXECUTIVE SUMMARY

The prevalence of lithium batteries is a potential hazard to aircraft safety. Lithium primary and secondary battery cells have the potential to undergo a process called thermal runaway. Thermal runaway causes an uncontrolled ion exchange, which can result in a rapid rise in temperature and pressure accompanied by the venting of flammable gases. This gas mixture along with the cell's high energy release can result in a fire and/or explosion. The hazards can vary by state of charge (SOC), cell chemistry, cell size, and other contributing factors. This study's design was to create a framework for potential guidelines for a standardized test method for the classification of a cell's hazard due to thermal runaway. Two initiation methods were examined—overcharging and overheating. Additionally, this study examined overheating with various heating rates.

The test article was a 21.7 L pressure vessel equipped with thermocouples and pressure transducers. The thermocouples measured the ambient and cell case temperature. Pressure transducers measured the pressure rise and quantified the gas release from the individual cells. The maximum cell case temperature, cell case temperature at the onset of thermal runaway, and peak percent pressure rise were measured. The thermal runaway vent gases were collected and analyzed for hydrogen, carbon monoxide, carbon dioxide, and hydrocarbon concentrations as a percent of total collected gases. The gas and pressure measurements determined the lower flammability limit (LFL) of the vent gas. The calculated LFL and total volume of the vent gas determined the maximum air-filled volume that becomes flammable per cell during thermal runaway.

Cylindrical lithium manganese dioxide (LiMnO_2) primary cells at 100% SOC, of type CR123a 3V 1500mAh, were tested. There were differences between the overheat method and the overcharge method. The methods varied by test duration, repeatability, and test results. The overheat method was the quickest and most repeatable method for producing a thermal runaway event. Overcharging cells was cumbersome and did not always produce thermal runaway.

Cylindrical lithium cobalt oxide (LiCoO_2) secondary cells at 30% SOC, of type 18650 3.7V 2600mAh, also were tested. Tests included heating the cells at 5°C/min, 10°C/min, 15°C/min, and 20°C/min. The results suggest that the heating rate significantly affects an 18650-sized cell's thermal runaway. A standardized test method should prescribe the heating rate. A critical threshold for a violent thermal runaway reaction was determined to be a maximum cell case temperature above 250°C and the release of over 0.5 L of vent gas. A heating rate of less than 12°C/min caused the 18650 cells to have a standard reaction. A heating rate of more than 17°C/min caused the cells to have a violent reaction. The LFL of the vent gas was 15.1% for a violent reaction and 12.0% for a standard reaction.

Pouch type LiCoO_2 secondary cells at 30% SOC, of size 5.4 x 47 x 95 mm 3.7V 2500mAh, also were tested. Tests included heating the cells at 5°C/min, 10°C/min, 15°C/min, 20°C/min, and 40°C/min. The results suggest that the heating rate moderately affects a pouch cell's thermal runaway. A standardized test method should prescribe the heating rate. For every 10 C°/min increase in heating rate, the total vent-gas volume increased by 0.057 L, the percent pressure rise increased by 0.89%, and the concentration of carbon dioxide decreased by 2.3%.

1. INTRODUCTION

1.1 BACKGROUND

Aircraft are commonly used to transport lithium-ion batteries. This creates a potential hazard for the passengers, crew members, and the aircraft. Lithium secondary and lithium primary battery cells can spontaneously go into thermal runaway. The hazard from thermal runaway can vary by state of charge (SOC), cell chemistry, cell size, and other contributing factors. Thermal runaway causes an uncontrolled ion exchange, which can result in a rapid rise in temperature and pressure accompanied by the venting of flammable gases. The cell's high energy release can cause flammable gases or materials to ignite and propagate fire. Additionally, the overpressure can cause structural damage to the aircraft. Between January 23, 2006, and January 22, 2020, 268 aviation cargo and passenger baggage events involving smoke, fire, extreme heat, or explosions involved lithium batteries (FAA, 2020).

1.2 OBJECTIVE

The objective of this study was to outline test procedures, measurements, and calculations to create a framework for potential guidelines for a standardized test method that determines a cell's hazard due to thermal runaway. Measured variables included the maximum cell case temperature, cell case temperature at the onset of thermal runaway, and peak percent pressure rise. The thermal runaway vent gases were collected and analyzed for hydrogen, carbon monoxide, carbon dioxide, and hydrocarbon concentrations as a percent of total collected gases. The gas and pressure measurements determined the LFL of the vent gas. The calculated LFL and total volume of the vent gas determined the maximum air-filled volume that becomes flammable per cell during thermal runaway.

Cylindrical LiMnO₂ primary cells at 100% SOC, of type CR123a 3V 1500mAh, were tested. Test methods to induce thermal runaway included the overheat method with and without a battery holder assembly and overcharging. This helped determine if the initiation method affects a cylindrical cell's hazard due to thermal runaway. Additionally, it helped determine if constricting cylindrical cells at the cathode and anode affects its thermal runaway.

Cylindrical LiCoO₂ secondary cells at 30% SOC, of type 18650 3.7V 2600mAh, also were tested. Tests included heating the cells at 5°C/min, 10°C/min, 15°C/min, and 20°C/min. This helped determine if the heating rate affects a cylindrical cell's hazard due to thermal runaway. This study similarly examined pouch type LiCoO₂ secondary cells at 30% SOC, of size 5.4 x 47 x 95 mm 3.7V 2500mAh. Tests included heating the cells at 5°C/min, 10°C/min, 15°C/min, 20°C/min, and 40°C/min. Likewise, this helped determine if the heating rate affects a pouch cell's hazard due to thermal runaway.

2. GENERAL TEST PROCEDURE

The test procedure followed the DOT/FAA/TC-15/59 Lithium Battery Thermal Runaway Vent Gas Analysis small-scale tests with a few modifications (FAA, 2016). A 21.7 L stainless-steel pressure vessel contained the tested individual battery cells (Figure 1). The vessel was semi-spherical and made of 316 L stainless steel. The wall thickness was 1.3 cm with an outside diameter of 32.4 cm. The pressure vessel had multiple ports for pressure transducers, gas lines, electrical pass-throughs, and thermocouples. Cells were 11.5 cm from the bottom of the sphere on top of an aluminum plate. A 1.6 mm type K thermocouple (Omega KQCL 1/16") located 9 cm above the cell measured the ambient temperature.

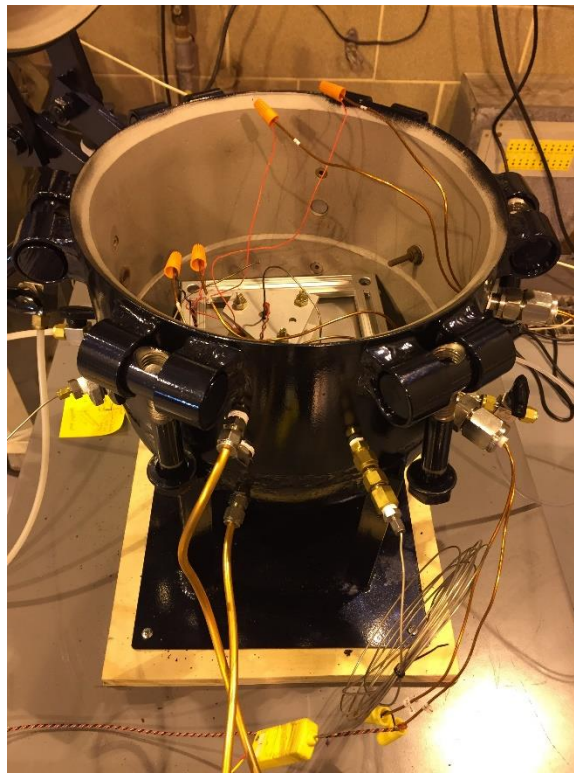


Figure 1. Test apparatus: 21.7 L pressure vessel used for testing

A vacuum pump evacuated the sealed pressure vessel to less than 0.7kPa. Then, a nitrogen bottle inserted 101.3kPa of nitrogen gas into the pressure vessel. Nitrogen gas has inert properties and does not interfere with the gas analyzers. The inert properties of nitrogen are important to retain the flammable gases for measurement. Either overcharging or overheating forced the individually tested cells into thermal runaway. A pressure transducer quantified the pressures generated from thermal runaway vent gases and measured the pressure spikes. The percent pressure-rise calculations used the difference of the maximum pressure and the original pressure divided by the original pressure (Equation 1).

$$\%P_R = \frac{P_m - P_{om}}{P_{om}} \quad (1)$$

Where:

$\%P_R$ = Percent pressure rise (%)

P_m = Maximum measured pressure (kPa)

P_{om} = Measured pressure before thermal runaway (kPa)

Each test recorded the post-thermal runaway pressure after the ambient temperature returned to its approximate pre-thermal runaway temperature. Gay-Lussac's Law accounted for small temperature differences in the pressure vessel (Equation 2). The thermal runaway vent-gas volume calculations used Boyle's Law with the recorded pre- and post-thermal runaway pressures and the volume of the pressure vessel (Equation 3).

$$P_o = P_{om} * \frac{273.15 + T_F}{273.15 + T_o} \quad (2)$$

Where:

P_o = Temperature-adjusted pressure before thermal runaway (kPa)

T_F = Ambient temperature after thermal runaway (°C)

T_o = Ambient temperature before thermal runaway (°C)

$$V_{vg} = \frac{P_f * V_{pv}}{P_o} - V_{pv} \quad (3)$$

Where:

V_{vg} = Vent gas volume (L)

V_{pv} = Pressure vessel volume (L)

P_f = Pressure after thermal runaway (kPa)

Then additional nitrogen gas filled the pressure vessel to 124kPa. This addition allows the gases to mix and creates a positive pressure to force the mixed vent gas into the gas analyzers. Gas chromatography with a thermal conductivity detector and flame ionization detector measured hydrogen and hydrocarbon concentrations. The nondispersive infrared radiation sensor measured carbon monoxide and dioxide concentration. The vent-gas composition calculations used Dalton's Law with the pressure measurements and the gas analyzers' measurements (Equations 4-6).

$$X_{vg} = \frac{P_f - P_o}{P_{F_2}} \quad (4)$$

Where:

X_{vg} = Percentage of vent gas by volume (% vol)

P_{F_2} = Pressure after thermal runaway with additional nitrogen addition (kPa)

$$X_{C_{vg}} = \frac{X_{C_{vg+N_2}}}{X_{vg}} \quad (5)$$

Where:

$X_{C_{vg}}$ = Percentage of a measured constituent in vent gas by volume (% vol)

$X_{C_{vg+N_2}}$ = Percentage of a measured constituent in vent gas and nitrogen by volume (% vol)

$$V_{C_{vg}} = X_{C_{vg}} * V_{vg} \quad (6)$$

Where:

$V_{C_{vg}}$ = Volume of vent gas constituent (kPa)

2.1 LE CHATELIER'S MIXING RULE

Le Chatelier's mixing rule accurately calculates the flammability limits of mixtures containing hydrogen, carbon monoxide, methane, and simpler paraffin hydrocarbons (Karp, 2016). However, calculated flammability limits are less accurate in mixtures containing vapors such as ether or acetone (Coward & Jones, 1952). Therefore, the mixing rule should not be used indiscriminately (Coward & Jones, 1952).

The method for calculating the flammability limits of mixed gases follows (Equation 7) (Coward & Jones, 1952):

1. Calculate the constituents of the mixed gas without air.
2. Create binary gases by combining part or all of a nonflammable gas with one or more flammable gases and then recalculate the gas constituents.
3. Record the flammability limits of the mixtures' constituents from tables or curves.
4. Calculate the flammability limits of the mixture using Le Chatelier's mixing rule equation.

$$L = \frac{100}{\frac{p_1}{N_1} + \frac{p_2}{N_2} + \frac{p_3}{N_3} + \dots} \quad (7)$$

Where L is either the LFL or the UFL of the gas mixture, p_1, p_2, p_3, \dots are the percentages of the mixture's constituents, and N_1, N_2, N_3, \dots are either the LFL or UFL of the individual constituents, respectively. Note that this study used the actual total percentage when the constituents did not add up to 100 percent.

2.2 MAXIMUM FLAMMABLE AIR-FILLED VOLUME PER CELL

This study estimated the maximum air-filled volume that will be flammable during thermal runaway per cell. The calculated average LFL and the measured average volume of thermal runaway vent gas determined the estimation (Equation 8).

$$MFA = \frac{V_{vg}}{LFL} * 100 \quad (8)$$

Where:

MFA = Maximum flammable airspace volume per cell (L)

LFL = Low flammability limit

2.3 STATISTICAL ANALYSIS

A two-sample t-test compares the means of two control groups (Montgomery, 2013). The test statistically determines if changing an independent variable of the control groups significantly affects the dependent variable. For example, this study compared the thermal runaway reaction of 18650 sized cells for heating rates below 15°C/min and at or above 15°C/min. The heating rate is the independent variable, and the thermal runaway reaction is the dependent variable. This test statistically determines if changing the heating rate affects the cell's thermal runaway reaction.

A one-way analysis of variance (ANOVA) test compares the means of two or more control groups (Montgomery, 2013). Each of the control groups has a different independent variable and a similar dependent variable. Similarly to the two-sample t-test, the ANOVA test statistically determines if changing the independent variable of the control groups significantly affects the dependent variable. For example, this study compared the thermal runaway reaction for three initiation methods. The initiation methods are the independent variable, and the thermal runaway reaction is the dependent variable. The ANOVA test statistically determines if the initiation method affects the thermal runaway reaction. However, the test does not compare the individual control groups to each other. A Tukey post-hoc test compares individual control groups to each other to determine if the altered independent variable significantly affects the dependent variable (Montgomery, 2013). For example, this test will determine if the initiation method A significantly affects the thermal runaway reaction when compared to initiation method B or initiation method C and so forth.

These statistical analysis tests assume the independence of observation, a normally distributed response variable, and homogeneity of variance (Montgomery, 2013).

2.3.1 OVERHEAT AND OVERCHARGE METHOD COMPARISON

Three initiation methods forced CR123a 3V 1500mAh LiMnO₂ cylindrical primary cells at 100% SOC into thermal runaway. The three initiation methods were:

- Overheat method with a battery holder assembly (Figure 2)
- Overheat method without a battery holder assembly (Figure 3)

- Overcharge method with a modified battery holder assembly (Figure 4)

The battery holder assembly assisted in measuring the cell's voltage for the overheat method. Additionally, it assisted in applying a charge for the overcharge method. The battery holder assembly consists of two pieces of nonconductive plates covering the cell's anode and the cathode (Figure 2 and Figure 4). The modified battery holder assembly used a spring between the positive terminal of the cell and the nonconductive plate (Figure 4). This enabled the venting mechanism to function properly.

A 20W polyimide film heater (Omega KHLV-102/10-P) was wrapped around the individual CR123a cells for the two overheat methods. A fastened 1.6mm type K thermocouple measured the temperature at the vertical center of the cell case (Figure 2 and Figure 4). The thermocouple was not in contact with the film heater. The cell was heated at 5-10 °C/min until thermal runaway occurred. Thermal runaway became evident with rapid self-induced temperature rise and a spike in pressure.

A direct current (DC) power supply (McMaster-Carr 7686K29) was used to power the individual cells for the overcharge method. Tested overcharge methods included:

- Incremental voltage increase with extended rest periods
- Incremental voltage increase with 30-minute rest periods
- Constant current input

Charging the cell to 6V and holding for five hours, followed by two days rest without charge, and then charging to 30V forced the cell into thermal runaway. Increasing the charge from 6V to 30V with 6V increments and 30-minute rest cycles also forced the cell into thermal runaway. Maintaining a constant charge rate of 1C and 3C did not force thermal runaway. With the constant current input, the positive thermal coefficient (PTC) current limiting switch activated and caused a non-energetic failure.

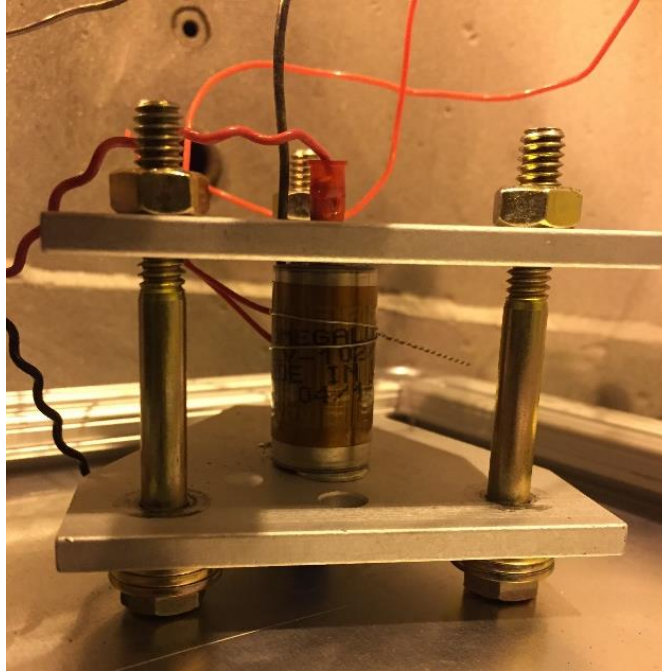


Figure 2. Overheat with battery holder assembly – CR123a cell



Figure 3. Overheat without battery holder assembly – CR123a cell

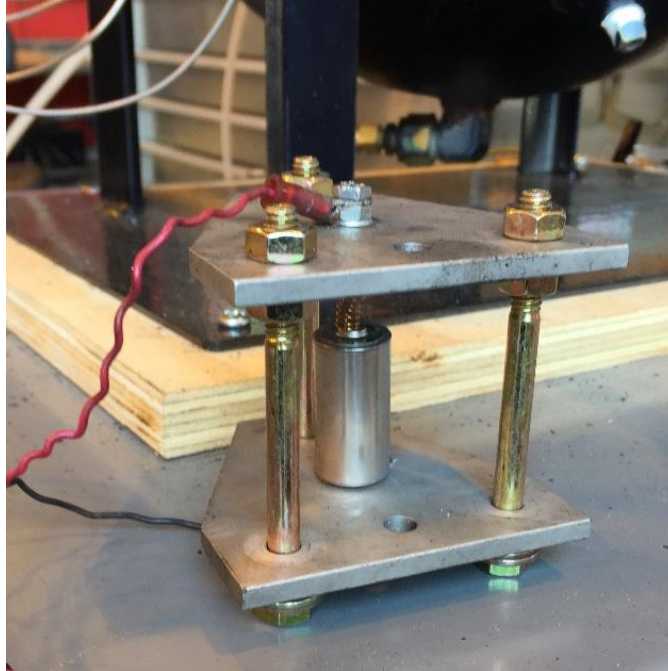


Figure 4. Overcharge with modified battery holder assembly – CR123a cell

2.4 HEATING RATE COMPARISON TEST PROCEDURE

This study experimented with pouch and cylindrical style lithium-ion cells to determine the effects of heating rate on a cell's thermal runaway. These two cell styles were:

- Cylindrical LiCoO₂ secondary cells at 30% SOC, of type 18650 3.7V 2600mAh
- Pouch LiCoO₂ secondary cells at 30% SOC, 5.4 x 47 x 95 mm 3.7V 2500mAh

A 40W polyimide film heater (Omega KHLV-202/10-P) wrapped around the individual 18650 cells for the overheat method (Figure 5). A fastened 1.6mm type K thermocouple measured the temperature at the vertical center of the cell case. The thermocouple was not in contact with the film heater.

A 160W polyimide film flexible heater (Omega KH-404/10-P) was placed under the individual pouch cells for the overheat method (Figure 6). A type K surface thermocouple with a self-adhesive backing (SA3-K-SRTC) measured the temperature at the side of the pouch cell. The pouch cell's side measured the greatest maximum temperature compared to the pouch cell's top and on the pouch cell's tab while being heated at 10°C/min (Figure 7). This best characterizes a pouch cell's internal temperature and potential hazard due to thermal runaway. Therefore, the pouch cell tests used the temperature measurements at the side of the pouch.

The film heater heated the individual cells at 5°C/min, 10°C/min, 15°C/min, 20°C/min, or 40°C/min until thermal runaway occurred. A proportional-integral-derivative (PID) controller (Omega CN1504-1507) controlled the heating rate. Figure 8 and Figure 9 grouped individual tests by the prescribed heating rate. Although the PID controller yielded reproducible results, there were

slight variances in the actual heating rate. This is more evident at high heating rates because of thermal lag (Figure 8 and Figure 9). Heaters with a greater heat flux could reduce thermal lag. The slope of the cell case temperature vs. time graph from 30 to 140°C calculated the actual heating rate. The statistical analysis used the actual heating rate while graphical representations used the prescribed heating rate.



Figure 5. Overheat setup – 18650 cell

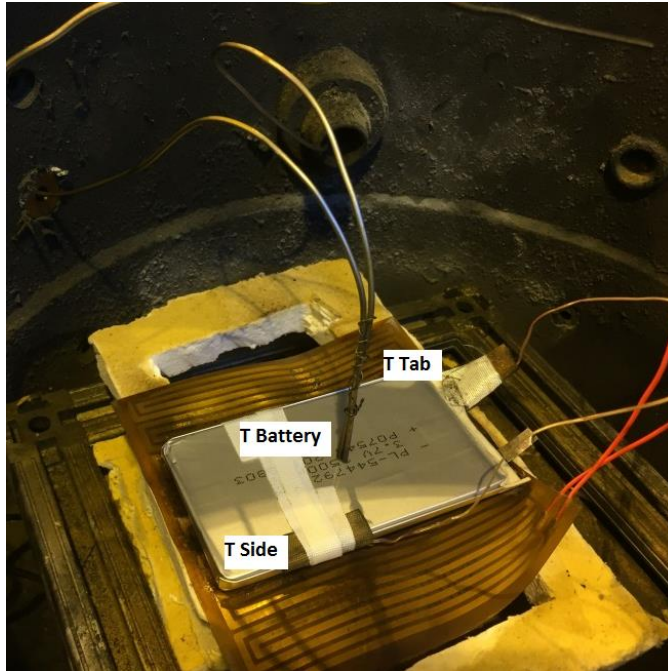


Figure 6. Cell thermocouple location – pouch cell

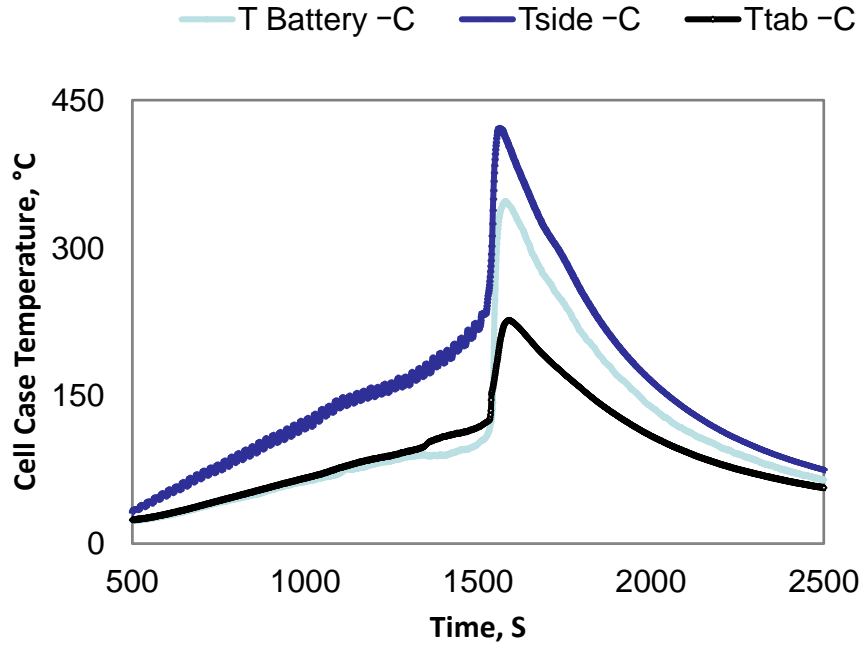


Figure 7. Cell case temperature versus time by thermocouple location at 10°C/min – pouch cell

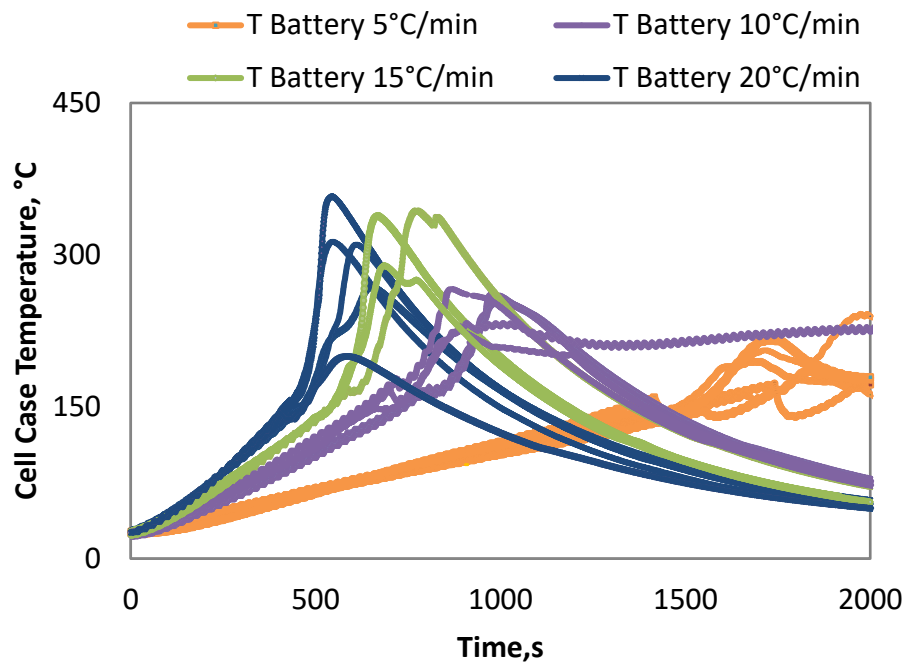


Figure 8. Cell case temperature versus time by heating rate – 18650 cell

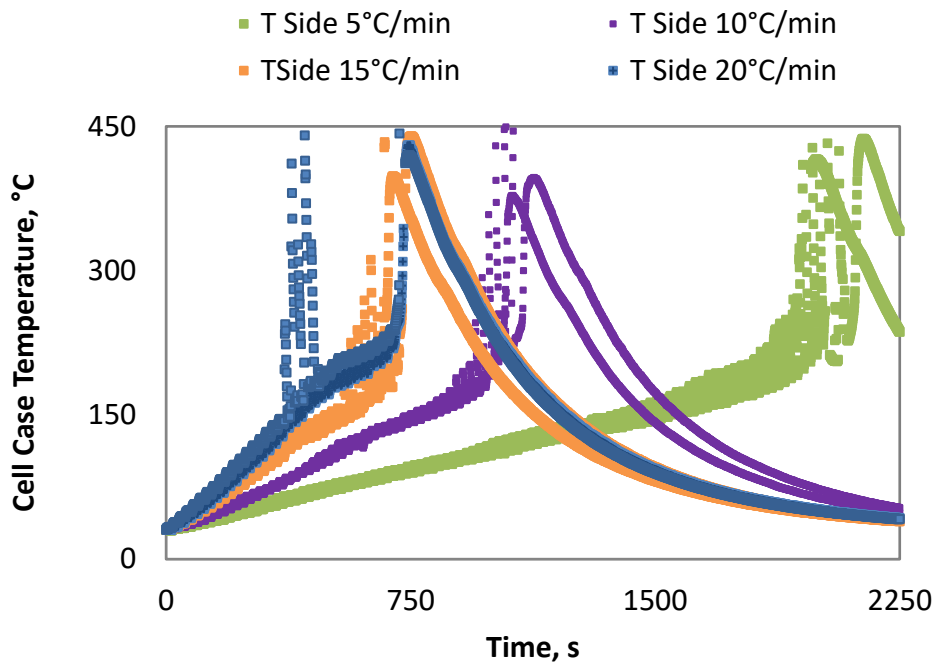


Figure 9. Cell case temperature versus time by heating rate – pouch cell

3. DISCUSSION OF RESULTS – OVERHEAT AND OVERCHARGE METHOD COMPARISON – CR123A CELL

Cylindrical LiMnO₂ primary cells at 100% SOC, of type CR123a 3V 1500mAh, were tested. Test methods to induce thermal runaway included the overheat method with and without a battery holder assembly and overcharging. This helped determine if the overheat method and the overcharge method affect a cylindrical cell's thermal runaway. Additionally, it helped determine if constricting cylindrical cells at the cathode and anode affects its thermal runaway.

3.1 INITIATION METHODS POST TEST VISUAL EXAMINATION – CR123A CELL

Three initiation methods forced CR123a 3V 1500mAh LiMnO₂ cylindrical primary cells at 100% SOC into thermal runaway. The three initiation methods were:

- Overheat method with a battery holder assembly (Figure 2)
- Overheat method without a battery holder assembly (Figure 3)
- Overcharge method with a modified battery holder assembly (Figure 4)

Altering the initiation method changed the thermal runaway event. Overheating the cell with the battery holder assembly caused the cell to fragment (Figure 10). The battery holder assembly constricted the venting mechanism. This prevented the venting mechanism from activating and caused the pressure inside to increase and explode. Overheating the cell without a battery holder assembly allowed the cell's venting mechanisms to activate. This prevented the cell from fragmenting (Figure 11).



Figure 10. Thermal runaway by overheating with battery holder assembly – CR123a cell

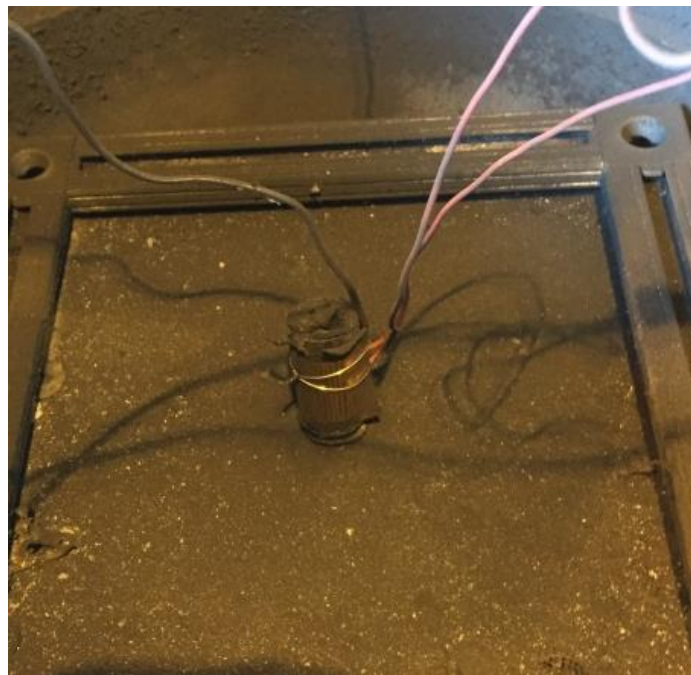


Figure 11. Thermal runaway by overheating without battery holder assembly – CR123a cell

Experimental observations were recorded where a DC power supply was used to overcharge the cells. Tested methods included:

- Incremental voltage increase with extended rest periods
- Incremental voltage increase with 30-minute rest periods
- Constant current input

The two methods using incremental voltage increase with rest periods caused thermal runaway. These methods caused the release of large quantities of vent gas through a small pin-sized hole near the positive side of the cell (Figure 12). The constant current input method activated the PTC current limiting switch and caused a non-energetic failure. The cell deformed and vented low quantities of gas but did not cause a rapid rise in temperature or pressure (Figure 13).



Figure 12. Deformation of cell casing due to thermal runaway by overcharging – CR123a cell



Figure 13. Deformation of cell casing due to energetic failure by overcharging – CR123a cell

3.2 VOLTAGE DURING OVERHEAT – CR123A CELL

The battery holder assembly helped record the voltage while overheating. The voltage increased from 3.17V to 3.24V as the cell's temperature increased (Figure 14). The voltage dropped to 0V before thermal runaway, and the voltage increased to 0.25V after thermal runaway. The voltage did not provide a clear and early indication of thermal runaway. Therefore, voltage measurements were abandoned.

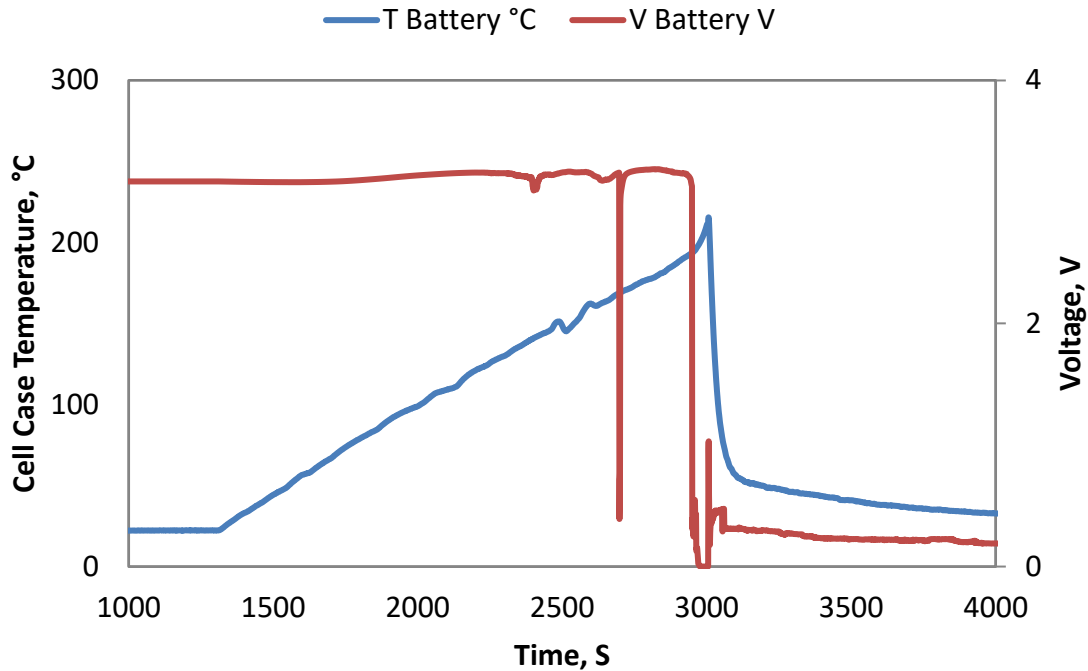


Figure 14. Cell case temperature and voltage output versus time - CR123a cell

3.3 METHODS AND THERMAL RUNAWAY ONSET TEMPERATURE – CR123A CELL

The thermal runaway onset temperature is the cell case temperature when apparent and rapid self-heating initiates. A one-way ANOVA test compared the effect of the initiation methods on the thermal runaway onset temperature ($F(2, 5) = 58.0, p = 0.003$). The low p-value suggests that the initiation method significantly affects the thermal runaway onset temperature (Figure 15). A Tukey post-hoc test revealed that there was a significant difference in the thermal runaway onset temperature between the overcharge method ($M = 88.8^\circ\text{C}, SD = 19.1^\circ\text{C}$) and the overheat method with a battery holder assembly ($M = 214^\circ\text{C}, SD = 2.12^\circ\text{C}, p = 0.001$). There also was a significant difference between the overcharge method and the overheat method without a battery holder assembly ($M = 187^\circ\text{C}, SD = 2.83^\circ\text{C}, p = 0.001$). There was no statistical difference in the thermal runaway onset temperature between the overheat method with or without the battery holder assembly ($p = 0.27$).

P-values less than 0.05 suggest that the initiation method affects the thermal runaway onset temperature, whereas p-values greater than 0.05 suggest the opposite. The results indicate that the test method can affect the thermal runaway onset temperature. Specifically, the low p-values suggest that the overcharge method is very likely to decrease the thermal runaway onset temperature compared to both of the overheat methods. The overcharge method heated from within. This might be the reason for the lower cell case temperature at the onset of thermal runaway. The high p-value suggests that constricting the venting mechanism did not affect the thermal runaway onset temperature.

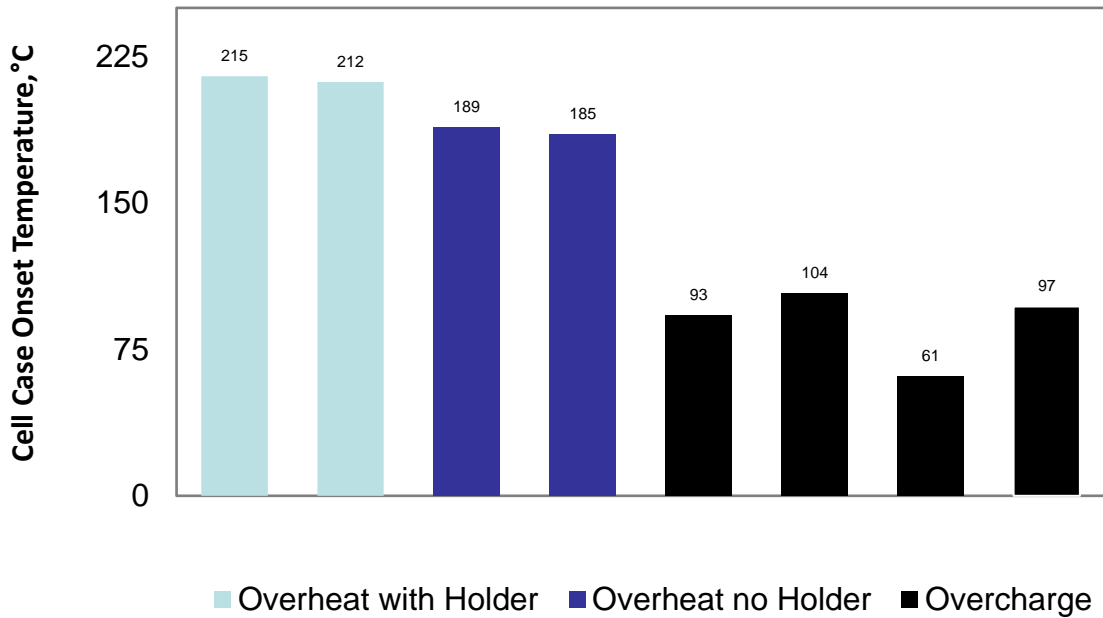


Figure 15. Thermal runaway onset temperature versus method – CR123a cell

3.4 METHODS AND MAXIMUM CELL CASE TEMPERATURE – CR123A CELL

High temperatures can cause flammable gases and surfaces to auto-ignite. A two-sample t-test compared the maximum cell case temperature for the overheat method without a battery holder assembly and the overcharge method (Figure 16). The maximum cell case temperature for the overheat method with a battery holder assembly was not measured because the cell fragmented upon thermal runaway. There was a very significant difference in the maximum cell case temperature for the overheat method with a battery holder assembly ($M=338$, $SD=29.7$) and the overcharge method ($M=493$, $SD=36.3$); $t(4) = 5.2$, $p = 0.0067$. The low p-value suggests that the test method does affect the maximum cell case temperature. Specifically, the results suggest that the overcharge method is very likely to increase the maximum cell case temperature. The added charge might have increased the cell's potential energy before releasing it during thermal runaway.

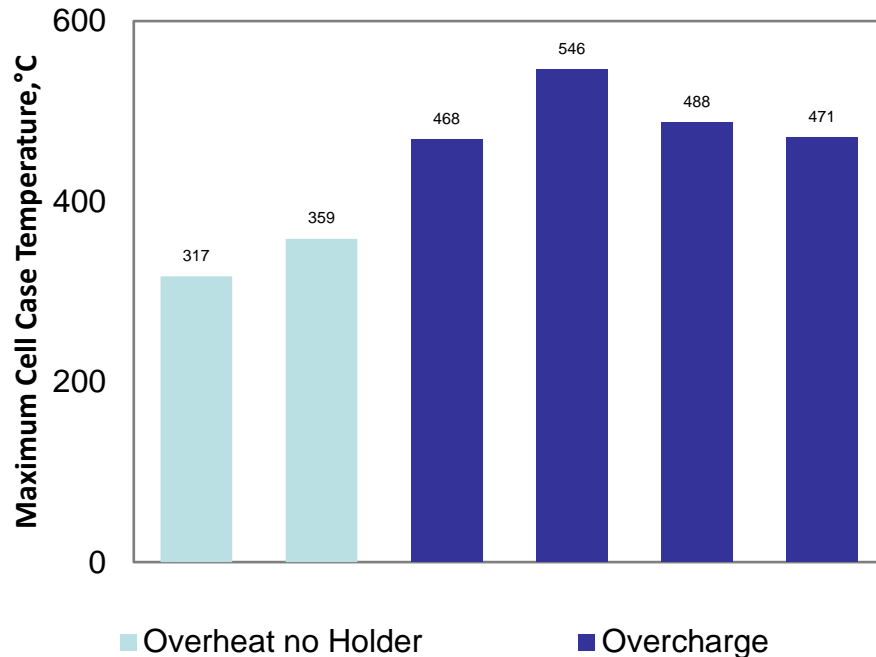


Figure 16. Maximum cell case temperature versus method – CR123a cell

3.5 METHODS AND VENT GAS VOLUME – CR123A CELL

A lithium battery cell vents a flammable gas mixture during thermal runaway. A one-way ANOVA test compared the effect of initiation methods on the vent gas volume ($F(2, 5) = 37.0, p = 0.001$). The low p-value suggests that the initiation method significantly affects the thermal runaway vent gas volume (Figure 17). A Tukey post-hoc test revealed that there was a significant difference in the thermal runaway vent gas volume between the overcharge method ($M = 2.88 \text{ L}, SD = 0.28 \text{ L}$) and the overheat method with a battery holder assembly ($M = 1.36 \text{ L}, SD = 0.03 \text{ L}, p = 0.001$). There also was a significant difference between the overcharge method and the overheat method without a battery holder assembly ($M = 1.75 \text{ L}, SD = 0.14 \text{ L}, p = 0.005$) (Figure 17). There was no statistical difference in the thermal runaway vent gas volumes between the overheat method with or without the battery holder assembly ($p = 0.28$).

P-values less than 0.05 suggest that the initiation method affects the thermal runaway vent gas volume, whereas p-values greater than 0.05 suggest the opposite. The results indicate that the test method can affect the thermal runaway vent gas volume. Specifically, the low p-values suggest that the overcharge method very likely increases the thermal runaway vent gas volume compared to both of the overheat methods. The overcharge method might have yielded the greatest volume of thermal runaway vent gas volume because of the added charge. The high p-value indicates that constricting the venting mechanism did not affect the thermal runaway vent gas volume.

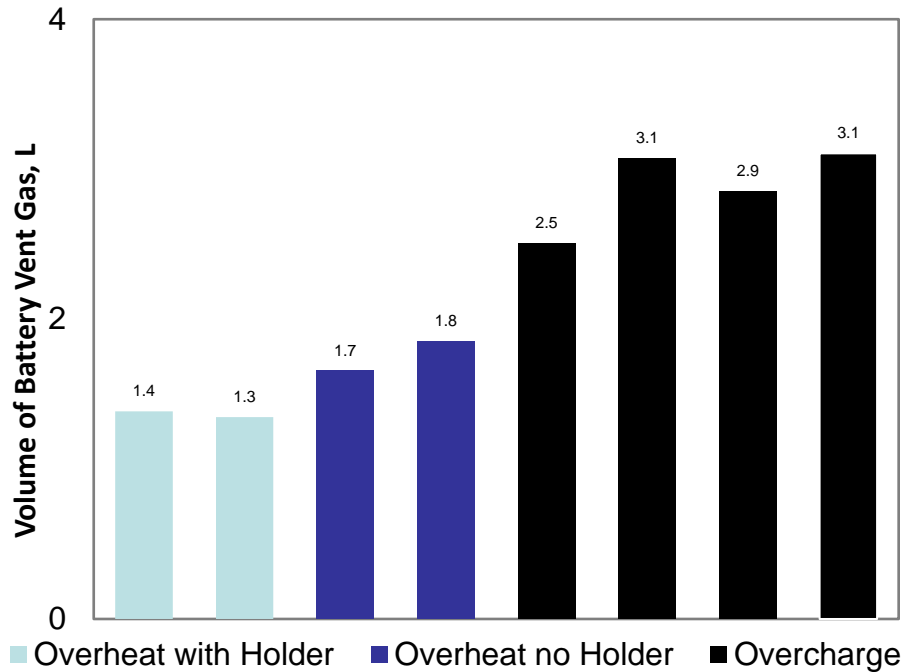


Figure 17. Vent gas volume versus method – CR123a cell

3.6 METHODS AND PERCENT PRESSURE RISE – CR123A CELL

Overpressure can cause structural damage to an aircraft and result in catastrophic system failure. A one-way ANOVA test compared the effect of initiation methods on the percent pressure rise ($F(2, 5) = 12.3, p = 0.012$). The low p-value suggests that the initiation method significantly affects the percent pressure rise (Figure 18). A Tukey post-hoc test revealed that there was a significant difference in the percent pressure rise between the overheat method with a battery holder assembly ($M = 86.9\%, SD = 10.1\%$) and the overheat method without a battery holder assembly ($M = 47.2\%, SD = 15.8\%, p = 0.04$). There also was a significant difference between the overheat method with a battery holder assembly and the overcharge method ($M = 36.8\%, SD = 10.6\%, p = 0.01$). There was no statistical difference in the percent pressure rise between the overheat method without a battery holder assembly and the overcharge method ($p = 0.6$).

P-values less than 0.05 suggest that the initiation method affects the percent pressure rise, whereas p-values greater than 0.05 suggest the opposite. The results indicate that the test method can affect the percent pressure rise. Specifically, the low p-values suggest that the overheat method with the battery holder assembly likely increases the percent pressure rise compared to both the overcharge method and the overheat method without the battery holder assembly. The overheat method with the battery holder assembly had the highest percent pressure rise because of the blocked venting mechanism. This caused the pressure inside the cell to build and explode. The high p-value indicates that there is no statistical difference in the percent pressure rise between the overheat method without the battery holder assembly and the overcharge method.

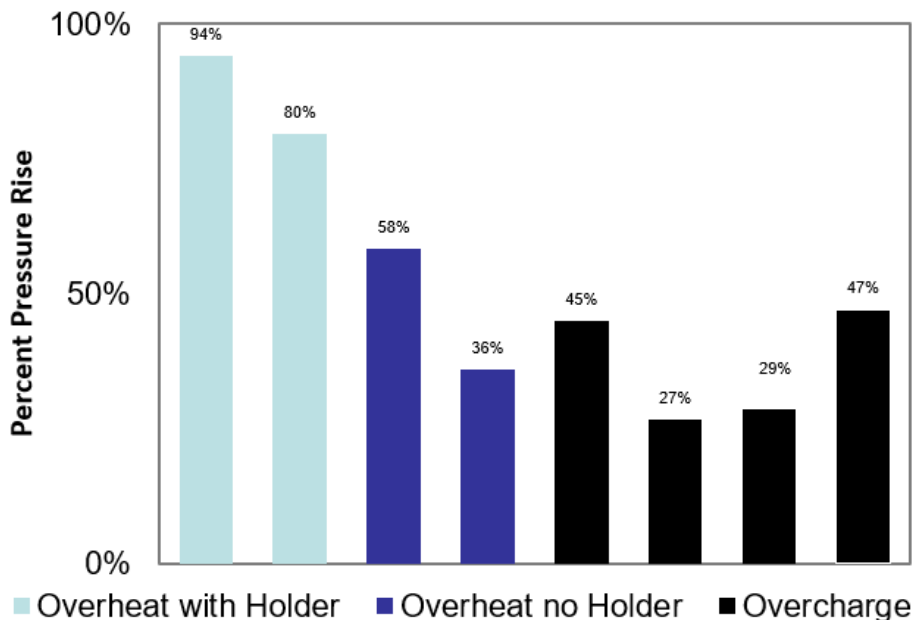


Figure 18. Percent pressure rise versus method – CR123a cell

3.7 METHODS AND TOTAL HYDROCARBON CONTENT – CR123A CELL

A one-way ANOVA test compared the effect of initiation methods on the total hydrocarbon content (THC) ($F(2, 5) = 48.3, p = 0.0005$). The low p-value suggests that the initiation method significantly affects the THC (Figure 19). A Tukey post-hoc test indicated that there was a significant difference in the vent gas THC between the overcharge method ($M = 16.4\%, SD = 1.1\%$) and the overheat method with a battery holder assembly ($M = 24.2\%, SD = 0.82\%, p = 0.001$). There was a significant difference between the overcharge method and the overheat method without a battery holder assembly ($M = 24.0\%, SD = 1.4\%, p = 0.001$). There was no statistical difference in the vent gas THC between the overheat method with or without the battery holder assembly ($p = 0.90$).

P-values less than 0.05 suggest that the initiation method affects the vent gas THC, whereas p-values greater than 0.05 suggest the opposite. The results indicate that the test method can affect the vent gas THC. Specifically, the low p-values suggest that the overcharge method very likely decreases the vent gas THC compared to both of the overheat methods. The high p-value indicates that constricting the venting mechanism did not affect the vent gas THC.

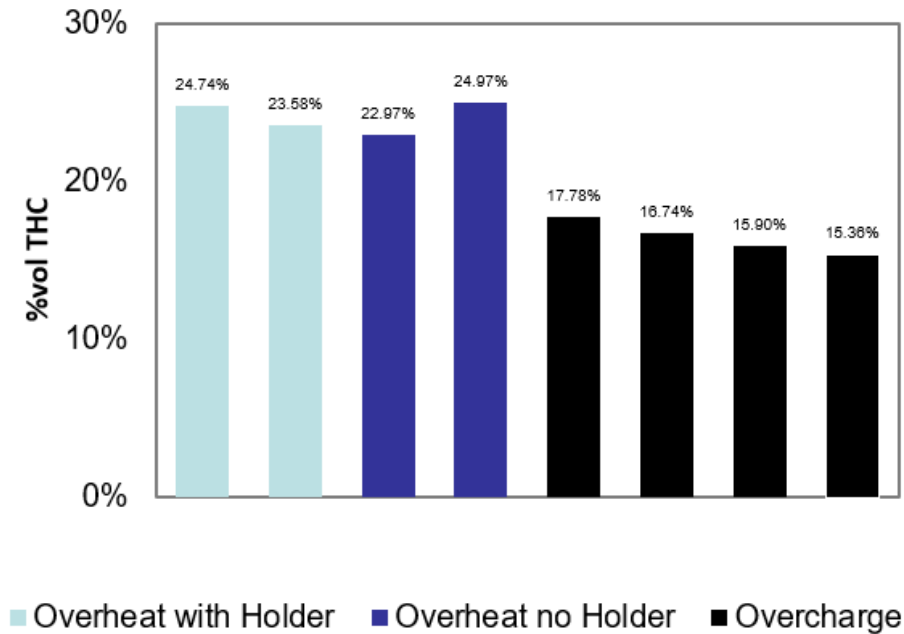


Figure 19. Total hydrocarbon content versus method– CR123a cell

4. DISCUSSION OF RESULTS - HEATING RATE COMPARISON – 18650 CELL

Cylindrical LiCoO₂ secondary cells at 30% SOC, of type 18650 3.7V 2600mAh, were tested. Tests included heating the cells at 5°C/min, 10°C/min, 15°C/min, and 20°C/min. This helped determine if the heating rate affects a cylindrical cell's thermal runaway.

4.1 HEATING RATE AND THERMAL RUNAWAY ONSET TEMPERATURE – 18650 CELL

The thermal runaway onset temperature is the cell case temperature when apparent and rapid self-heating initiates. A two-sample t-test compared the thermal runaway onset temperature for heating rates below 15°C/min and at or above 15°C/min (Figure 20). There was no statistical difference in the thermal runaway onset temperature for heating rates below 15°C/min ($M=158^{\circ}\text{C}$, $SD=12^{\circ}\text{C}$) and heating rates at or above 15°C/min ($M=150^{\circ}\text{C}$, $SD=9^{\circ}\text{C}$); $t(20)=1.8$, $p=0.086$. The high p-value suggests that the heating rate does not affect the cell case temperature at the onset of thermal runaway.

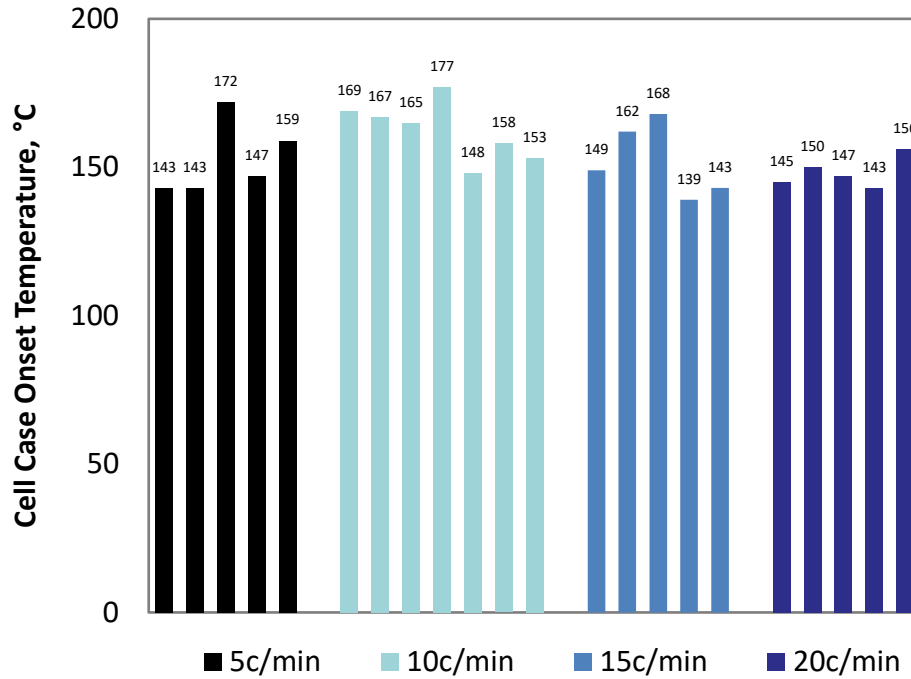


Figure 20. Thermal runaway onset temperature versus heating rate – 18650 cell

4.2 HEATING RATE AND MAXIMUM CELL CASE TEMPERATURE – 18650 CELL

A two-sample t-test compared the maximum cell case temperature for heating rates below 15°C/min and at or above 15°C/min. There was a very significant difference in the maximum thermal runaway case temperature for heating rates below 15°C/min ($M=228^{\circ}\text{C}$, $SD=35^{\circ}\text{C}$) and heating rates at or above 15°C/min ($M=288^{\circ}\text{C}$, $SD=54^{\circ}\text{C}$); $t(20) = 3.1$, $p = 0.0053$. The results suggest that the heating rate significantly affects the maximum thermal runaway cell case temperature. Specifically, our results suggest that heating rates at or above 15°C/min are very likely to increase the maximum cell case temperature. Temperatures above 250°C occurred in 0/5 (0%) tests at 5°C/min, 3/7 (43%) tests at 10°C/min, 4/5 (80%) tests at 15°C/min, and 4/5 (80%) tests at 20°C/min (Figure 21).

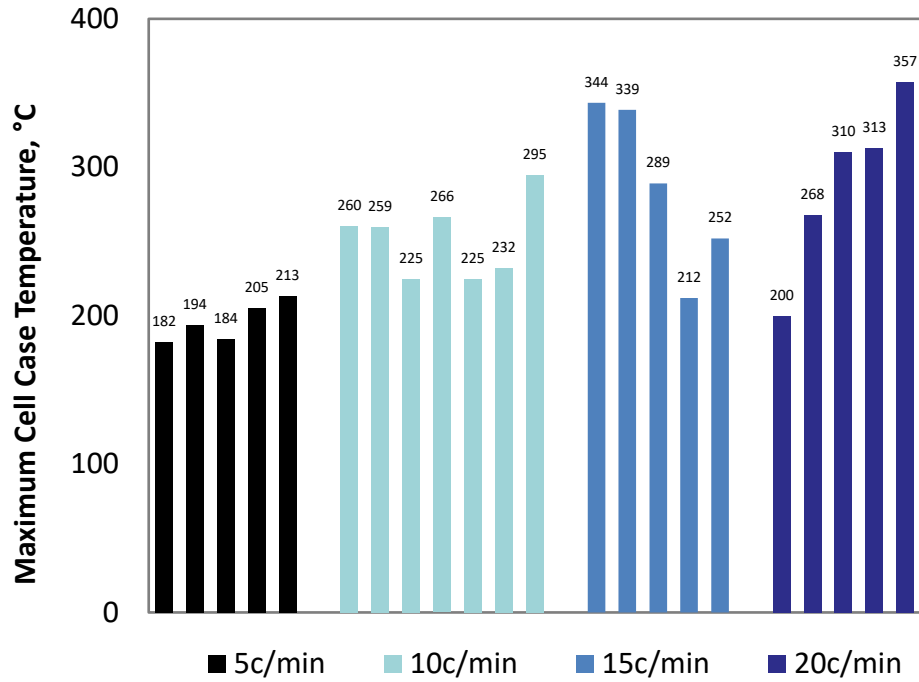


Figure 21. Maximum cell case temperature versus heating rate – 18650 cell

4.3 HEATING RATE AND VENT GAS VOLUME – 18650 CELL

A two-sample t-test compared the thermal runaway vent gas for heating rates below 15°C/min and at or above 15°C/min. There was an extremely significant difference in the volume of the vent gas for heating rates below 15°C/min ($M=0.38$ L, $SD=0.055$ L) and heating rates at or above 15°C/min ($M=0.57$ L, $SD=0.14$ L); $t(20) = 4.3$, $p = 0.0003$. The low p-value strongly suggests the heating rate affects the thermal runaway vent gas. Specifically, heating rates at or above 15°C/min are extremely likely to increase the volume of thermal runaway vent gas. Over 0.5 L of vent gas occurred in 0/5 tests (0%) at 5°C/min, 1/7 tests (14%) at 10°C/min, 3/5 tests (60%) at 15°C/min, and 4/5 tests (80%) at 20°C/min (Figure 22).

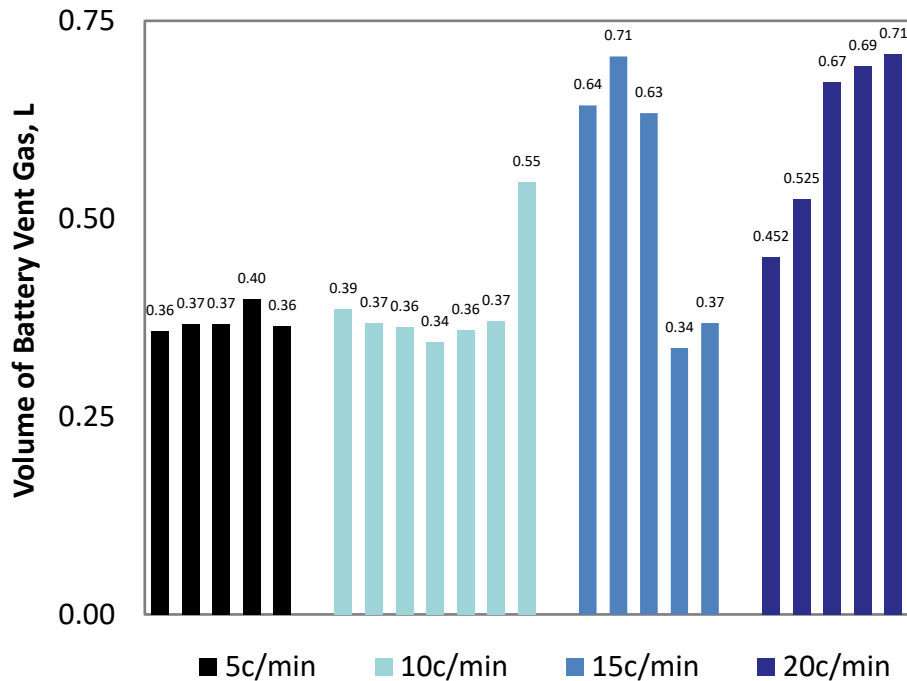


Figure 22. Vent gas volume versus heating rate – 18650 cell

4.4 HEATING RATE AND REACTION TYPE – 18650 CELL

A critical threshold for a violent thermal runaway reaction was determined to be a maximum cell case temperature above 250°C and the release of over 0.5 L of vent gas. The threshold is not intended to be universal and would likely change with other cells and states of charge. This study uses the threshold to demonstrate how the heating rate affects the measurements of hazards due to thermal runaway. Heating rates at or above 15°C/min were more likely to produce a violent thermal runaway reaction with both the heat and vent gas requirements. Violent reactions occurred in 0/5 tests (0%) at 5°C/min, 1/7 tests (14%) at 10°C/min, 3/5 tests (60%) at 15°C/min, and 4/5 tests (80%) at 20°C/min (Figure 23). Reactions that produced over 0.5 L of vent gas also measured a maximum cell case temperature of over 250°C. However, reactions that measured a maximum cell case temperature over 250°C did not always produce over 0.5 L of vent gas. The heating rate did not affect the thermal runaway onset temperature. Therefore, slower heating rates allow more time for the electrolyte inside of the cells to boil and vent than faster heating rates. This infers that more of the electrolyte remains in the form of potential energy for tests with faster heating rates.

The heating rate was a significant factor in determining how an 18650 cell reacted during thermal runaway. However, there was an overlapping range in heating rate from 12.8 to 16.4°C/min that a mix of standard and violent thermal runaway reactions occurred (Figure 24). A heating rate of less than 12°C/min caused the 18650 cells to have a standard reaction. A heating rate greater than 17°C/min caused the cells to have a violent reaction. Therefore, a standardized test method should prescribe the heating rate to ensure consistent results. Additional tests need to verify if the heating rate boundaries and their relation to standard and violent thermal runaway reactions in 18650 cells at 30% SOC translate to other cylindrical lithium-ion cells and states of charge.

This study grouped test results by reaction type to determine the differences between standard and violent thermal runaway reactions. The analysis included the reactions' maximum cell case temperature, total vent-gas volume per cell, percent pressure rise, hydrogen volume, and carbon dioxide volume (Table 1 through Table 7).

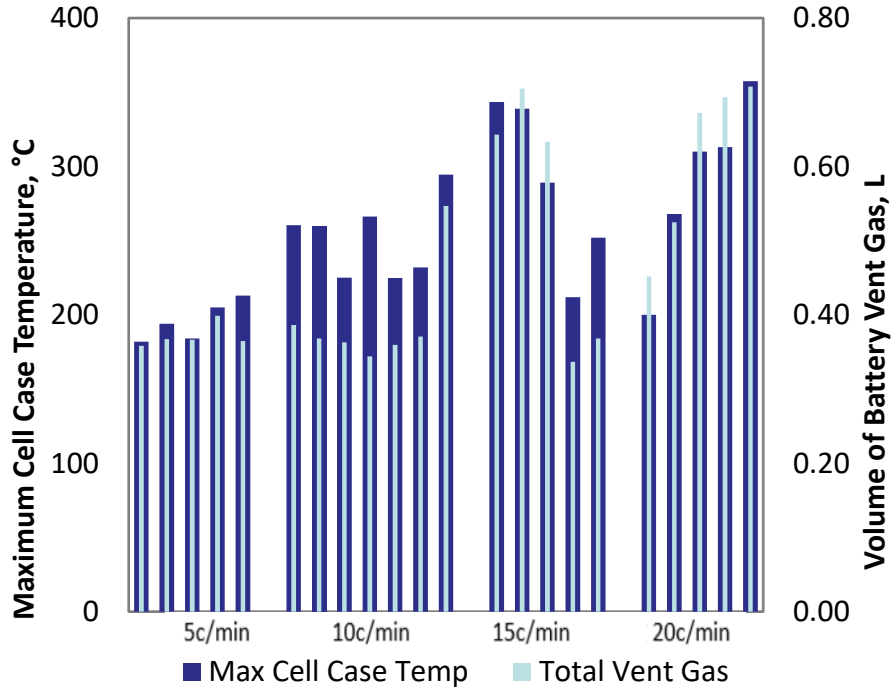


Figure 23. Maximum cell case temperature and vent gas volume versus heating rate – 18650 cell

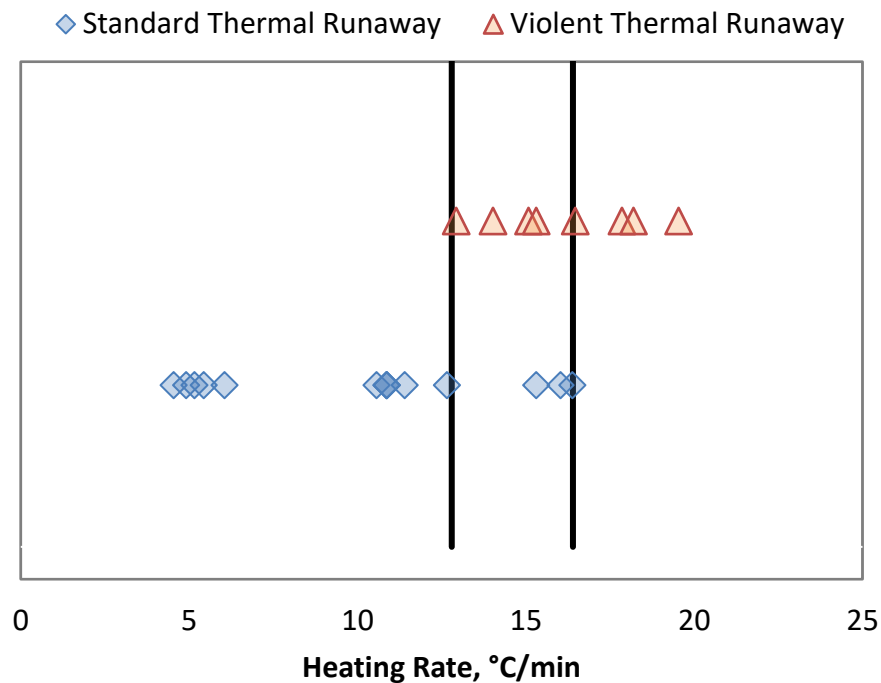


Figure 24. Reaction type versus heating rate – 18650 cell

4.5 REACTION TYPE AND MAXIMUM CELL CASE TEMPERATURE – 18650 CELL

High temperatures can cause flammable gases and surfaces to auto-ignite. There was a 34.3% difference in the maximum cell case temperature between a standard and a violent thermal runaway reaction (Table 1 and Figure 25). Violent thermal runaway reactions caused a greater maximum cell case temperature than standard thermal runaway reactions. The mean difference in the maximum cell case temperature was 92°C. There was a 95% confidence interval ranging from 64.9 to 119°C.

Table 1. Maximum cell case temperature and reaction type – 18650 cell

Reaction Type	Number of Tests	Maximum Cell Case Temperature, °C		
		Mean	SD	SEM
Standard	14	222	28.6	7.64
Violent	8	314	30.5	10.8

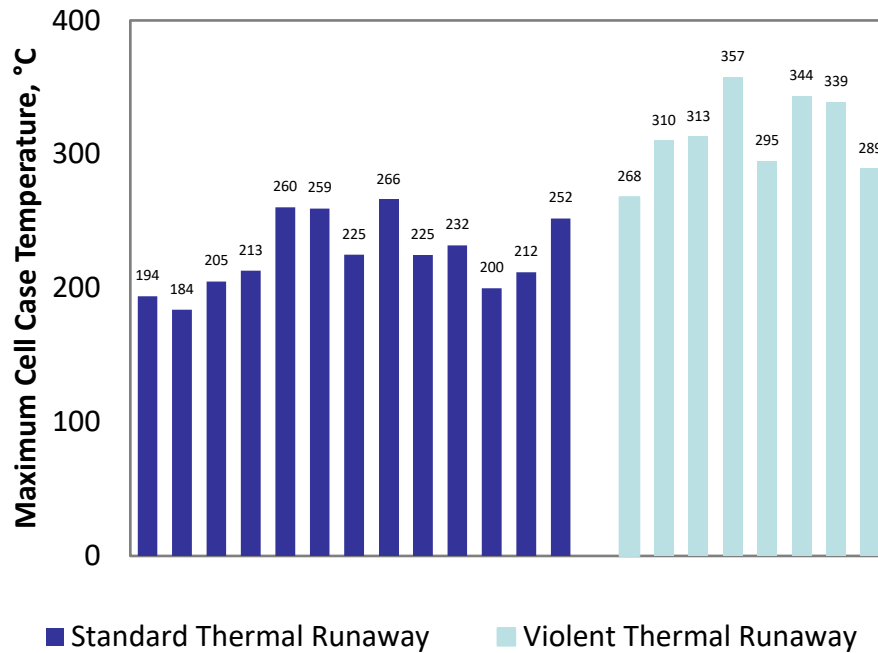


Figure 25. Maximum cell case temperature versus reaction type – 18650 cell

4.6 REACTION TYPE AND VENT GAS VOLUME – 18650 CELL

A lithium battery cell vents a flammable gas mixture during thermal runaway. There was a 53.5% difference in the thermal runaway vent gas volume between a violent and standard thermal runaway reaction (Table 2 and Figure 26). Violent thermal runaway reactions produced a greater volume of vent gas than standard thermal runaway reactions. The mean difference in vent gas volume was 0.27 L. There was a 95% confidence interval ranging from 0.22 to 0.31 L.

Table 2. Thermal runaway vent gas volume and reaction type – 18650 cell

Reaction Type	Number of Tests	Thermal Runaway Vent Gas Volume, L		
		Mean	SD	SEM
Standard	14	0.37	0.028	0.007
Violent	8	0.64	0.070	0.025

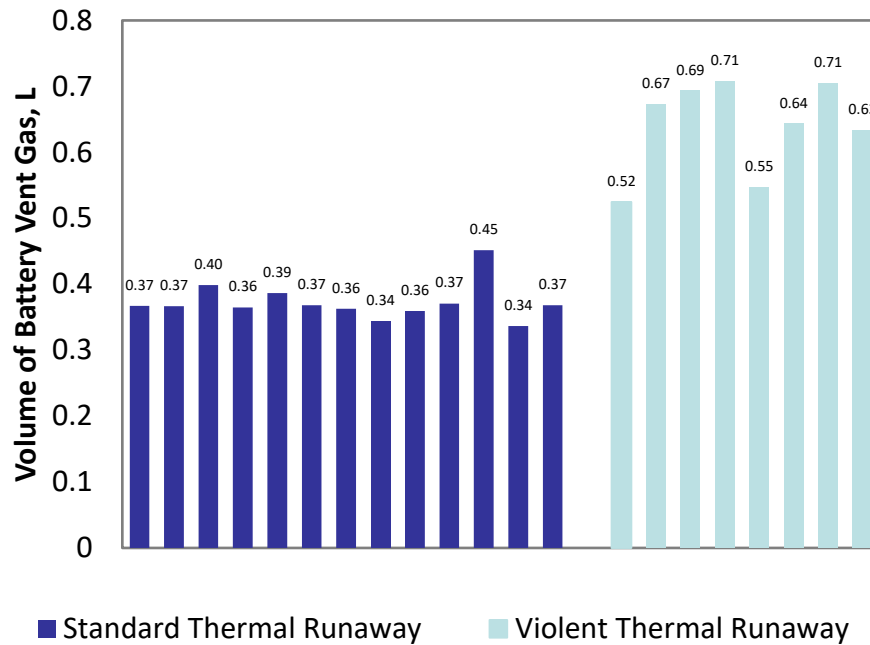


Figure 26. Cell vent gas volume versus reaction type – 18650 cell

4.7 REACTION TYPE AND PERCENT PRESSURE RISE – 18650 CELL

Overpressure can cause structural damage to an aircraft and result in catastrophic system failure. There was a 48.4% difference in the percent pressure rise between a standard and violent thermal runaway reaction. The mean difference in the percent pressure rise was 3.11% (Table 3 and Figure 27). Violent thermal runaway reactions caused a greater percent pressure rise than standard thermal runaway reactions. There was a 95% confidence interval ranging from 1.69 to 4.54%. The violent thermal runaway reaction had a maximum of 11.9% pressure rise. The standard thermal runaway had a maximum of 5.6%.

Table 3. Percent pressure rise and reaction type – 18650 cell

Reaction Type	Number of Tests	Percent Pressure Rise, %		
		Mean	SD	SEM
Standard	14	4.88	0.46	0.02
Violent	8	8.00	2.52	0.89

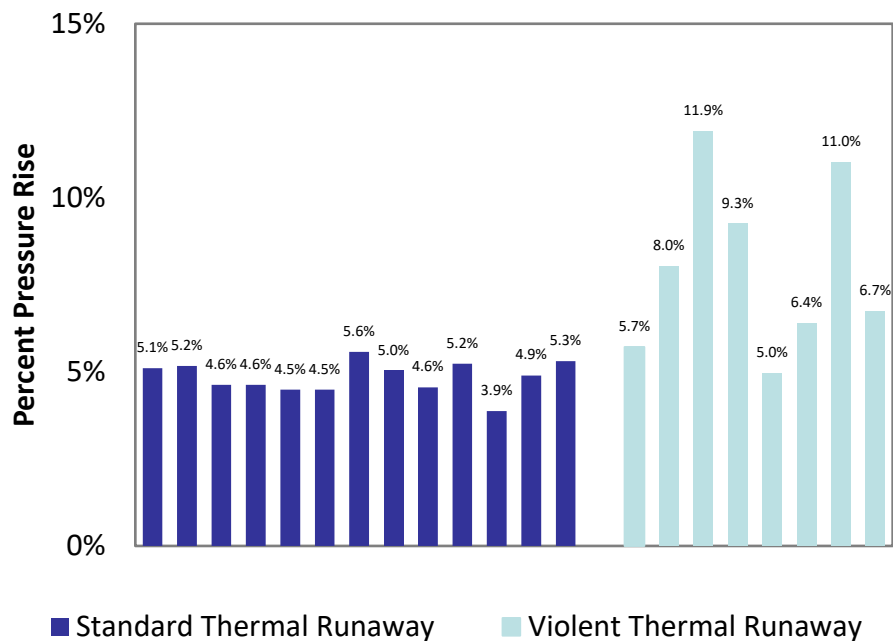


Figure 27. Percent pressure rise versus reaction type – 18650 cell

4.8 REACTION TYPE AND HYDROGEN CONCENTRATION – 18650 CELL

Hydrogen is a major contributor to the constituents of lithium-ion thermal runaway vent gas. Hydrogen has a wide flammability range from 4.95 to 76.5% by volume (Karp, 2016). There was a 53.1% difference in the hydrogen concentration between a standard and a violent thermal runaway reaction (Table 4 and Figure 28). Violent thermal runaway reactions produced a greater percent concentration of hydrogen than standard thermal runaway reactions. The mean difference in percent concentration of hydrogen was 4.26% by volume. There was a 95% confidence interval ranging from 2.76 to 5.77% by volume.

Table 4. Hydrogen concentration and reaction type – 18650 cell

Reaction Type	Number of Tests	Hydrogen Concentration, % vol		
		Mean	SD	SEM
Standard	11	5.98	1.45	0.44
Violent	5	10.3	0.80	0.36

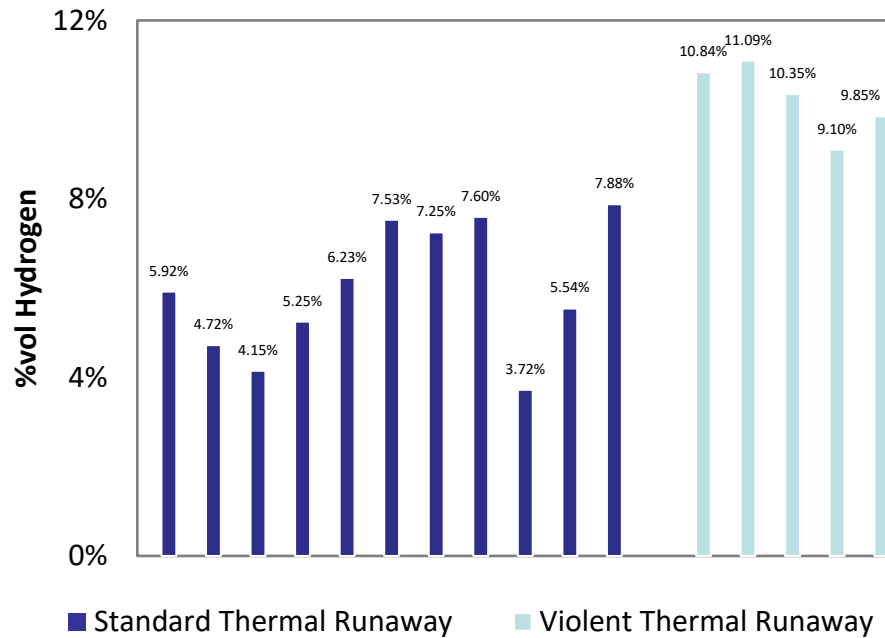


Figure 28. Hydrogen concentration versus reaction type – 18650 cell

4.9 REACTION TYPE AND TOTAL HYDROGEN VOLUME – 18650 CELL

There was a 101% difference in the total volume of hydrogen found in thermal runaway cell vent gas between a standard and a violent thermal runaway reaction (Table 5 and Figure 29). Violent thermal runaway reactions produced a greater volume of hydrogen than standard thermal runaway reactions. The mean difference in the total volume of hydrogen was 0.045 L. There was a 95% confidence interval ranging from 0.037 to 0.053 L.

Table 5. Hydrogen volume and reaction type – 18650 cell

Reaction Type	Number of Tests	Hydrogen Volume, L		
		Mean	SD	SEM
Standard	11	0.022	0.005	0.001
Violent	5	0.067	0.011	0.005

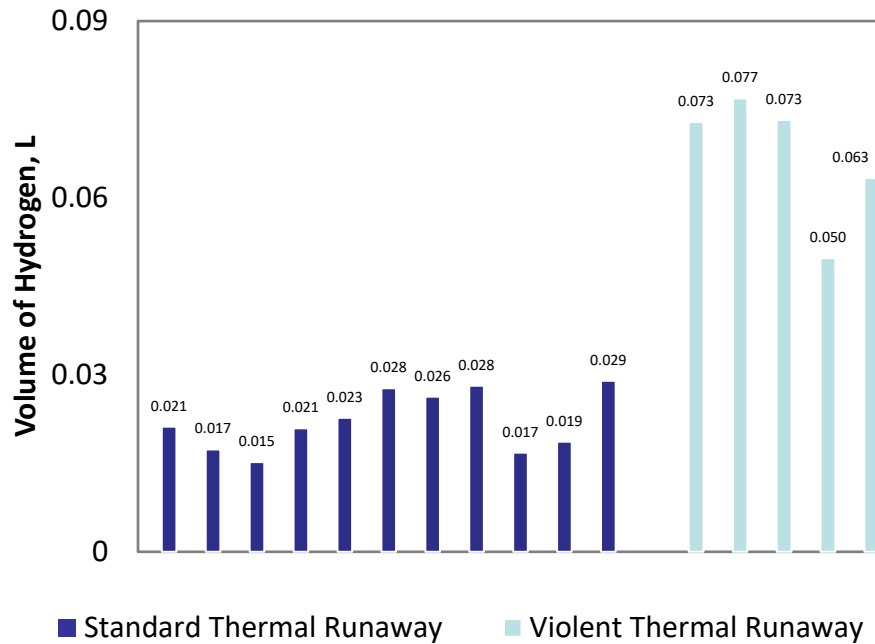


Figure 29. Total volume of hydrogen versus reaction type – 18650 cell

4.10 REACTION TYPE AND CARBON DIOXIDE CONCENTRATION – 18650 CELL

Carbon dioxide is a major contributor to the constituents of lithium-ion thermal runaway vent gases. Carbon dioxide is a non-poisonous and non-flammable gas. Carbon dioxide helps constrict the flammability limits of the thermal runaway vent gas mixture. There was a 67.4% difference in the carbon dioxide concentration between a standard and a violent thermal runaway reaction (Table 6 and Figure 30). Violent thermal runaway reactions produced a greater percent concentration of carbon dioxide than standard thermal runaway reactions. The mean difference in percent concentration of carbon dioxide was 17.6% by volume. There was a 95% confidence interval ranging from 12.6 to 22.6% by volume.

Table 6. Carbon dioxide concentration and reaction type – 18650 cell

Reaction Type	Number of Tests	Carbon Dioxide Concentration, % vol		
		Mean	SD	SEM
Standard	6	17.33	3.64	1.49
Violent	4	34.92	2.77	1.38

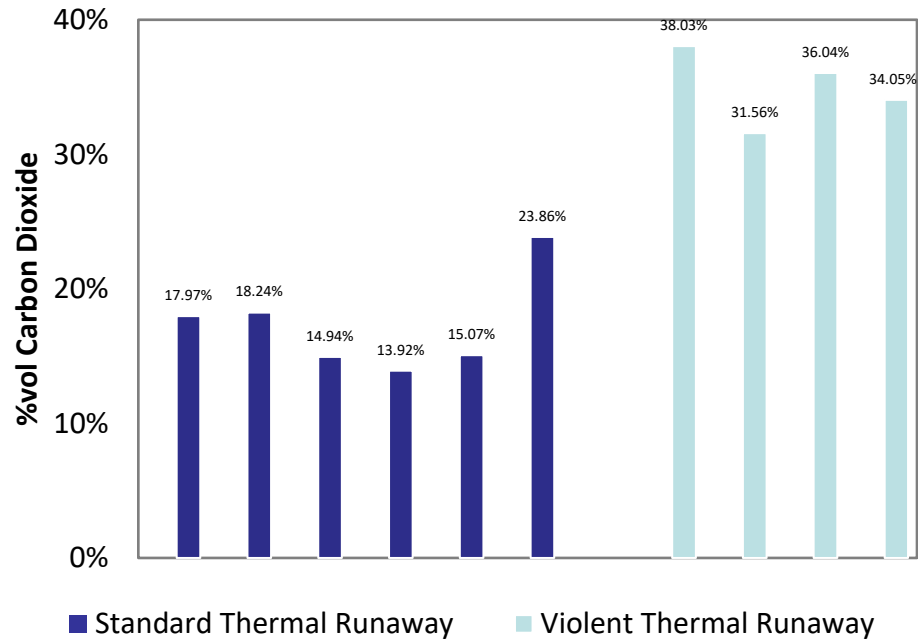


Figure 30. Concentration of carbon dioxide versus reaction type – 18650 cell

4.11 REACTION TYPE AND TOTAL CARBON DIOXIDE VOLUME – 18650 CELL

There was a 110% difference in the total volume of carbon dioxide found in thermal runaway cell vent gas between a standard and a violent thermal runaway reaction (Table 7 and Figure 31). Violent thermal runaway reactions produced a greater volume of carbon dioxide than standard thermal runaway reactions. The mean difference in the total volume of carbon dioxide was 0.16 L. There was a 95% confidence interval ranging from 0.12 to 0.20 L.

Table 7. Carbon dioxide total volume and reaction type – 18650 cell

Reaction Type	Number of Tests	Carbon Dioxide Volume, L		
		Mean	SD	SEM
Standard	6	0.063	0.015	0.006
Violent	4	0.22	0.040	0.020

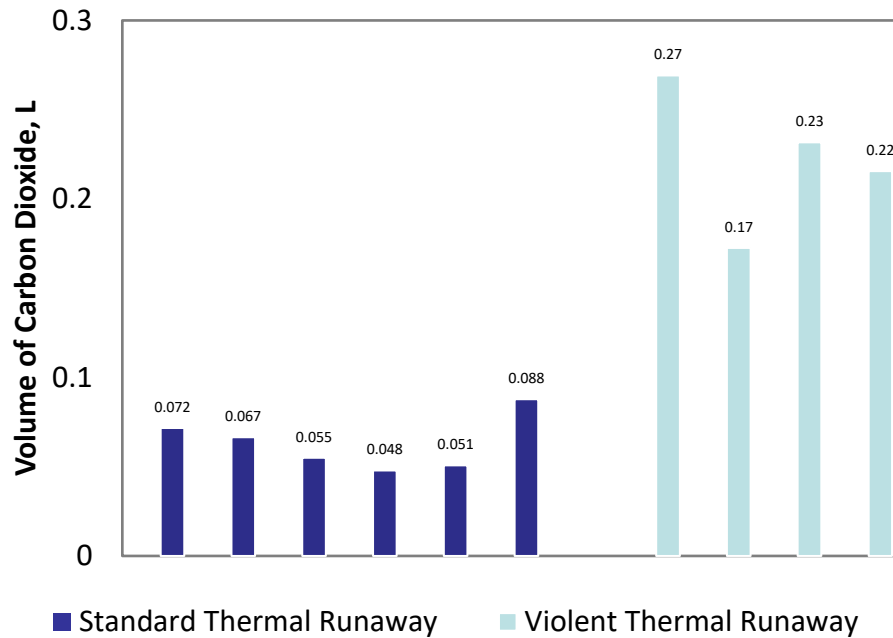


Figure 31. Carbon dioxide volume versus reaction type – 18650 cell

4.12 LE CHATELIER'S MIXING RULE CALCULATION – 18650 CELL

This study separated the gas concentrations used for the calculation of the LFL by reaction type (Table 8) (Karp, 2016) (Coward & Jones, 1952).

Table 8. Gas concentration and LFL – 18650 cell

Gas	Standard Thermal Runaway, % vol	Violent Thermal Runaway, % vol	LFL, % vol
carbon dioxide	17.33±2.91	34.92±2.71	NA
carbon monoxide	4.71±0.41	3.84±0.39	12.50
ethane	0.27±0.05	0.46±0.16	3.00
ethylene	2.16±0.45	1.67±0.24	3.10
hydrogen	5.98±0.86	10.30±0.70	4.95
methane	1.02±0.28	1.27±0.35	5.30
propane	0.10±0.01	0.14±0.07	2.10

propylene	0.07±0.01	0.26±0.18	2.40
-----------	-----------	-----------	------

± Confidence intervals based off of a 95% confidence interval

Standard thermal runaway reactions produced a more flammable gas mixture than violent thermal runaway reactions. The calculated LFL of the produced gases was 15.1±2.1% for a violent thermal runaway. The calculated LFL of the produced gases was 12.0±2.0% for a standard thermal runaway reaction. There was a 22.9% difference in the calculated LFL between a standard and a violent thermal runaway reaction.

Violent thermal runaway reactions produced a greater maximum air-filled volume that becomes flammable per cell than standard thermal runaway reactions despite its higher LFL. This is because a violent thermal runaway reaction produced 53% more vent gas than a standard thermal runaway reaction. The maximum air-filled volume that becomes flammable after a violent thermal runaway reaction was 4.23±1.04 L per cell for a violent thermal runaway reaction and 3.09±0.75 L per cell for a standard thermal runaway reaction. There was a 31.1% difference in the maximum volume of flammable cell vent gas and air mixture per cell between a standard and a violent thermal runaway reaction.

5. DISCUSSION OF RESULTS – HEATING RATE COMPARISON – POUCH CELL

Pouch type LiCoO₂ secondary cells at 30% SOC, of size 5.4 x 47 x 95 mm 3.7V 2500mAh, were tested. Tests included heating the cells at 5°C/min, 10°C/min, 15°C/min, 20°C/min, and 40°C/min. This helped determine if the heating rate affects a pouch cell's thermal runaway. An in-depth discussion of the thermal runaway onset temperature was not included for pouch cells. Yet it is worth noting that the heating rate did not affect the cell case temperature at the onset of thermal runaway.

5.1 HEATING RATE AND MAXIMUM CELL CASE TEMPERATURE – POUCH CELL

The mean maximum cell case temperature across all heating rates was 404°C (*SD*=36.9°C, *SEM*=13.0°C). A non-significant regression equation was found ($F(1, 8) = 0.56, p = 0.47$) with an R^2 of 0.06. The high p-value suggests that the heating rate did not affect the maximum cell case temperature (Figure 32). A hypothesized reason that the pouch cell's maximum cell-case temperatures were unaffected by the heating rate is that the soft case expanded to contain vent gases and electrolytes as they were heated to thermal runaway. This infers that a similar amount of electrolyte remained in the form of potential energy regardless of the heating rates.

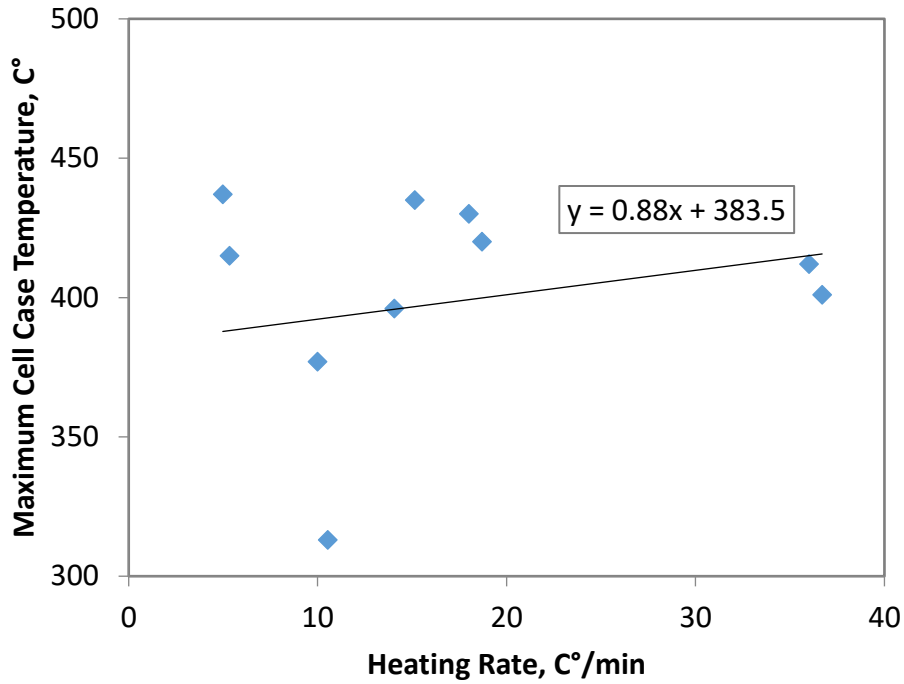


Figure 32. Maximum cell case temperature versus heating rate – pouch cell

5.2 HEATING RATE AND VENT GAS VOLUME – POUCH CELL

The mean volume of thermal runaway vent gas across all heating rates was 0.94 L ($SD=0.17$ L, $SEM=0.04$ L). A significant regression equation was found ($F(1, 9)=18.24$, $p=0.0016$) with an R^2 of 0.65. The p-value less than 0.005 suggest that the heating rate significantly affects the total vent gas volume. A simple linear regression predicted change in the vent gas volume based on the heating rate. The results suggest that as the heating rate increases by 1 C°/min, the vent gas volume should increase by 0.0057L. There was a 95% confidence interval ranging between 0.0027 to 0.0087 L per 1 C°/min (Figure 33).

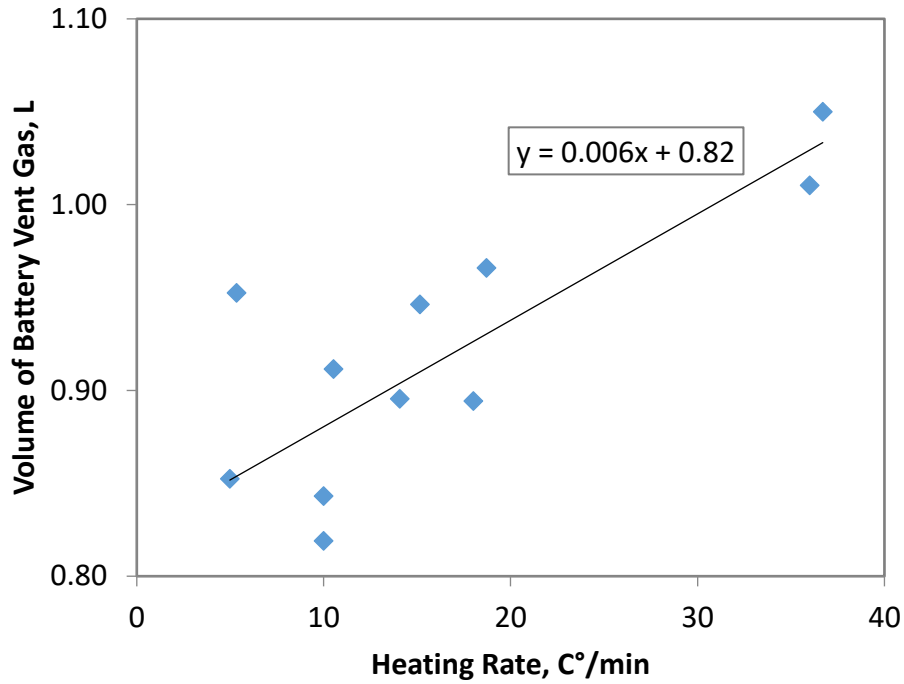


Figure 33. Total vent gas volume versus heating rate – pouch cell

5.3 HEATING RATE AND PERCENT PRESSURE RISE – POUCH CELL

The mean percent pressure rise across all heating rates was 20.6% ($SD=2.74\%$, $SEM=0.73\%$). A significant regression equation was found ($F(1, 8) = 9.24$, $p=0.016$), with an R^2 of 0.54. The p-value less than 0.05 suggests that the heating rate affects the percent pressure rise. A simple linear regression predicted the change in the percent pressure rise based on the heating rate. The results suggest that as the heating rate increases by 1 C°/min, the percent pressure rise should increase by 0.089%. There was a 95% confidence interval ranging between 0.022 to 0.157% per 1 C°/min (Figure 34).

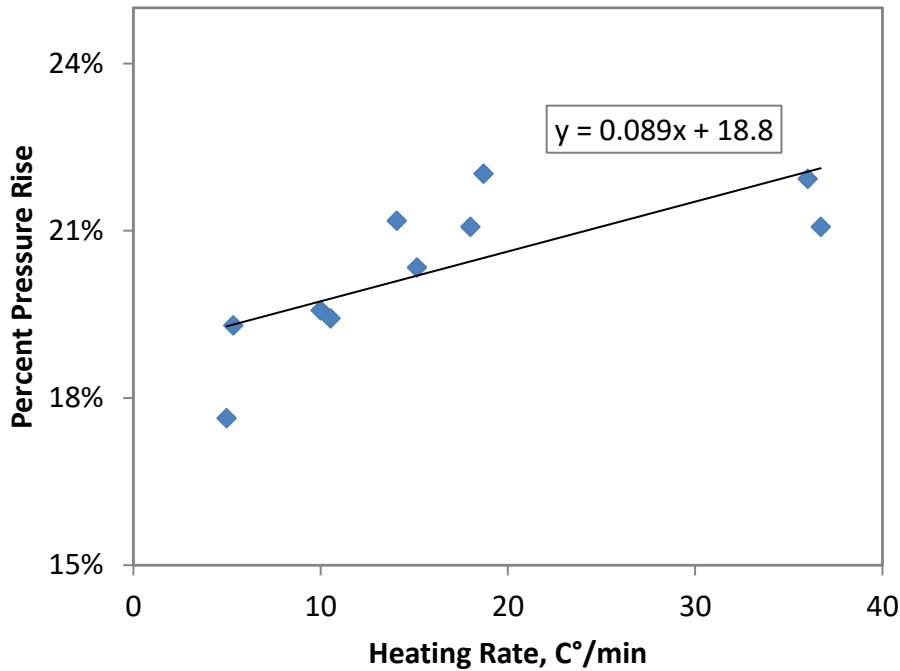


Figure 34. Percent pressure rise versus heating rate – pouch cell

5.4 HEATING RATE AND HYDROGEN CONCENTRATION – POUCH CELL

The mean concentration of hydrogen gas in a single thermal runaway event was 17.0% by volume ($SD=1.72\%$) with a 95% confidence interval ranging from 15.5 to 18.4% by volume. The heating rate did not significantly affect the hydrogen concentration in the thermal runaway vent gas.

5.5 HEATING RATE AND TOTAL HYDROGEN VOLUME – POUCH CELL

The mean volume for hydrogen gas in a single thermal runaway event was 0.16 L ($SD=0.03$ L). There was a 95% confidence interval ranging from 0.13 to 0.17 L. Heating rate did not significantly affect the total volume of hydrogen produced during thermal runaway.

5.6 HEATING RATE AND CARBON DIOXIDE CONCENTRATION – POUCH CELL

The mean concentration for carbon dioxide gas in a single thermal runaway event was 41.8% by volume ($SD=3.30\%$ by volume). There was a 95% confidence interval ranging from 39.5 to 44.2% by volume. A significant regression equation was found ($F(1, 8)=5.54, p=0.046$), with an R^2 of 0.41. A simple linear regression predicted the change in the concentration of carbon dioxide produced in a single cell venting based on the heating rate. The p-value of less than 0.05 suggests that the heating rate affects the concentration of carbon dioxide produced. The results suggest that as the heating rate increases by 1 C°/min, the concentration of carbon dioxide should decrease by 0.236%. There was a 95% confidence interval ranging between 0.00474 to 0.467% per 1 C°/min (Figure 35).

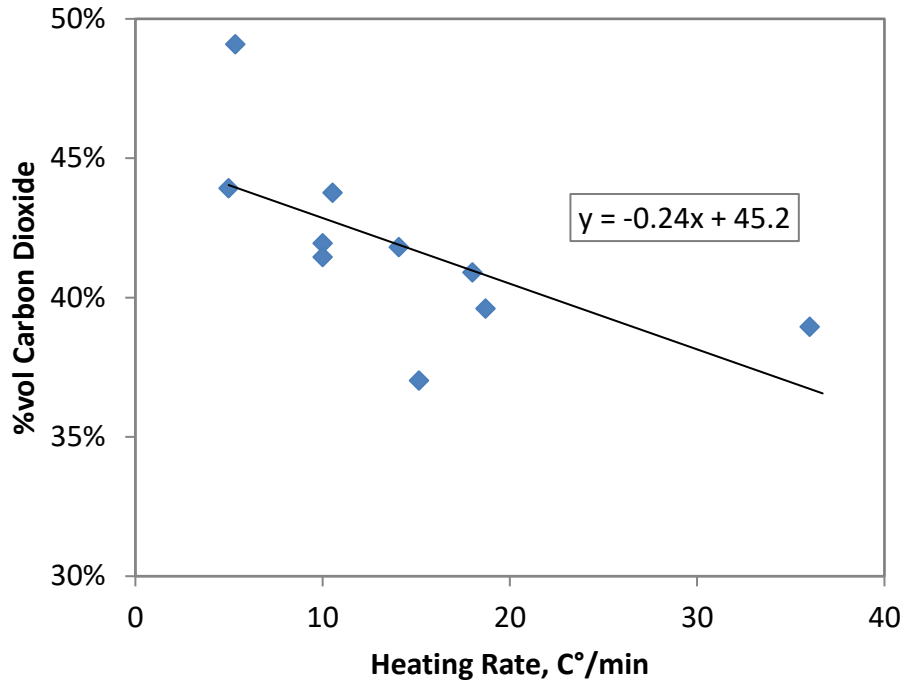


Figure 35. CO2 concentration vs heating rate – pouch cell

5.7 HEATING RATE AND TOTAL CARBON DIOXIDE VOLUME – POUCH CELL

The average volume of ten test results for carbon dioxide gas in a single thermal runaway event was 0.38 L ($SD=0.04$ L). There was a 95% confidence interval ranging from 0.35 to 0.41 L. Although the heating rate affected the concentration of carbon dioxide per thermal runaway event, the heating rate did not affect the volume of carbon dioxide per thermal runaway event. That is because the increase in the total volume of thermal runaway vent gas counteracted the decrease in the concentration of carbon dioxide as the heating rate increased.

5.8 LE CHATELIER’S MIXING RULE CALCULATION – POUCH CELL

This study separated the gas concentrations used for the calculation of the LFL by reaction type (Table 9) (Karp, 2016) (Coward & Jones, 1952).

Table 9. Gas concentration and LFL – Pouch cell

Gas	Averaged Gas Concentration, % vol	LFL, % vol
carbon dioxide	41.20±2.05	NA
carbon monoxide	3.82±0.35	12.50
ethane	1.35±0.08	3.00

ethylene	3.72±0.11	3.10
hydrogen	17.00±1.19	4.95
methane	2.58±0.09	5.30
propane	0.34±0.02	2.10
propylene	3.75±0.29	2.40

± Confidence intervals based on a 95% confidence interval

The LFL of the gases produced from a single 3.7V 2500mAh lithium-ion secondary pouch cell at 30% SOC during thermal runaway was 9.7%±0.7%. The estimated maximum air-filled volume that becomes flammable after thermal runaway came from the calculated LFL and the measured thermal runaway vent gas volume. The maximum air-filled volume that becomes flammable after a thermal runaway reaction was 9.7±1.6 L.

6. SUMMARY OF RESULTS

This study examined a potential standardized test method for the classification of a cell's hazard due to thermal runaway. Classifying a cell's hazards due to thermal runaway can help determine appropriate mitigation methods for the transport of batteries. The hazards can vary by SOC, cell chemistry, cell size, and other contributing factors. Table 10 summarizes the test results.

Cylindrical LiMnO₂ primary cells at 100% SOC, of type CR123a 3V 1500mAh, were tested. Test methods to induce thermal runaway included the overheat method with and without a battery holder assembly and overcharging. There were differences between the overheat method and the overcharge method. They varied by time to complete tests, consistency, and test results. The overheat method was the quickest and most consistent method for producing thermal runaway. Overcharging cells was cumbersome and did not always produce thermal runaway.

The battery holder assembly assisted in measuring the cell's voltage for the overheat method. Yet, the voltage did not provide a clear and early indication of thermal runaway. Furthermore, overheating the cell with the battery holder assembly prevented the cell's venting mechanism from activating. This caused the cell to fragment and made it impossible to measure the maximum cell case temperature. Additionally, it is important to note that it is unlikely that the cells would be situated in such a constricted manner during transport. Overheating the cell without a battery holder assembly allowed the venting mechanisms to activate and prevented it from fragmenting. For these reasons, later tests abandoned the battery holder assembly.

The overcharge method was very likely to decrease thermal runaway onset temperature compared to the overheat method. The overcharge method heated from within. Thus, it yielded the lowest case temperature at the onset of thermal runaway. Constricting the venting mechanism did not affect the thermal runaway onset temperature.

The overheat method with the battery holder assembly was likely to increase the percent pressure rise when compared to the overheat method without the battery holder assembly and the

overcharge method. The overheat method with the battery holder assembly constricted the venting mechanism. This caused the pressure inside to increase and explode. Thus, it had the highest percent pressure rise. Testing showed no statistical difference for the percent pressure rise between the overheat method without the battery holder assembly and the overcharge method.

The overcharge method was very likely to increase the thermal runaway vent gas volume compared to the overheat method. The overcharge method might have yielded the greatest volume of thermal runaway vent gas volume because of the added energy. Testing showed that a constricted venting mechanism did not affect the thermal runaway vent gas volume.

The overcharge method was very likely to decrease the THC compared to the overheat method. Testing showed that a constricted venting mechanism did not affect the THC in the thermal runaway vent gas composition.

Cylindrical LiCoO₂ secondary cells at 30% SOC, of type 18650 3.7V 2600mAh, also were tested. Tests included heating the cells at 5°C/min, 10°C/min, 15°C/min, and 20°C/min. The results suggest that the heating rate significantly affects an 18650-sized cell's thermal runaway. A standardized test method should prescribe the heating rate. Additional tests need to verify if the heating rate boundaries and their relation to standard and violent thermal runaway reactions in 18650 cells at 30% SOC translate to other cylindrical lithium-ion cells.

The thermal runaway onset temperature was the cell case temperature when apparent and rapid self-heating initiates. This study compared the thermal runaway onset temperature for heating rates below 15°C/min and at or above 15°C/min and found no statistical difference. However, there was a very significant difference in the maximum thermal runaway case temperature and total vent gas volume. The heating rate did not affect the thermal runaway onset temperature. Therefore, slower heating rates allow more time for the electrolyte inside of the cells to boil and vent than faster heating rates. This infers that more of the electrolyte remains in the form of potential energy.

A critical threshold for a violent thermal runaway reaction was determined to be a maximum cell case temperature above 250°C and the release of over 0.5 L of vent gas. The threshold is not intended to be universal and would likely change with other cells and states of charge. This study uses the threshold to demonstrate how the heating rate affects the measurements of hazards due to thermal runaway. Heating rates at or above 15°C/min were more likely to produce a violent thermal runaway reaction. Low p-values suggest that the heating rate is a significant factor in determining how an 18650 cell will react during thermal runaway. However, there was an overlapping range from 12.8 to 16.4°C/min that a mix of standard and violent thermal runaway reactions occurred. Heating rates less than 12°C/min caused the 18650 cells to have a standard reaction. Heating rates greater than 17°C/min caused the cells to have a violent reaction.

This study separated test results by reaction type to determine the differences between standard and violent thermal runaway reactions. Violent thermal runaway reactions caused a greater maximum cell case temperature than standard thermal runaway reactions. There was a 34.3% difference in the maximum cell case temperature between a standard and a violent thermal runaway reaction. The mean difference in the maximum cell case temperature was 92°C.

Violent thermal runaway reactions produced a greater volume of thermal runaway vent gas than standard thermal runaway reactions. There was a 53.5% difference in the thermal runaway vent gas volume between a violent and standard thermal runaway reaction. The mean difference in vent gas volume was 0.27 L.

Violent thermal runaway reactions caused a greater percent pressure rise than standard thermal runaway reactions. There was a 48.4% difference in the percent pressure rise between a standard and violent thermal runaway reaction. The mean difference in the percent pressure rise was 3.11%.

Violent thermal runaway reactions produced a greater volume of hydrogen than standard thermal runaway reactions. There was a 101% difference in the total volume of hydrogen found in the thermal runaway vent gas between a standard and a violent thermal runaway reaction. The mean difference in the total volume of hydrogen was 0.045 L.

Violent thermal runaway reactions produced a greater volume of carbon dioxide than standard thermal runaway reactions. There was a 110% difference in the total volume of carbon dioxide found in the thermal runaway vent gas between a standard and a violent thermal runaway reaction. The mean difference in the total volume of carbon dioxide was 0.16 L.

Standard thermal runaway reactions produced a more flammable gas mixture than violent thermal runaway reactions. The calculated average LFL of the vent gas was $15.1 \pm 2.1\%$ for a violent thermal runaway reaction and $12.0 \pm 2.0\%$ for a standard thermal runaway reaction. There was a 22.9% difference in the calculated LFL between a standard and a violent thermal runaway reaction.

Violent thermal runaway reactions produced a greater maximum air-filled volume that becomes flammable per cell than standard thermal runaway reactions. The maximum air-filled volume that becomes flammable after a violent thermal runaway reaction was 4.2 ± 1.0 L per cell, and 3.1 ± 0.8 L per cell for a standard thermal runaway reaction. There was a 31.1% difference in the maximum volume of flammable cell vent gas and air mixture per cell between a standard and a violent thermal runaway reaction.

Pouch type LiCoO₂ secondary cells at 30% SOC, of size 5.4 x 47 x 95 mm 3.7V 2500mAh, also were tested. Tests included heating the cells at 5°C/min, 10°C/min, 15°C/min, 20°C/min, and 40°C/min. The results suggest that the heating rate moderately affects a pouch cell's thermal runaway. A standardized test method should prescribe the heating rate. Additional tests need to verify if the test results from the tested pouch cells at 30% SOC translate to other pouch lithium-ion cells and SOC.

The heating rate did not significantly affect the thermal runaway onset temperature, maximum cell case temperature, and hydrogen concentration. However, low p-values suggest that the heating rate affects the total vent gas volume, percent pressure rise, and the concentration of carbon dioxide. Specifically, for every 10 C°/min increase in heating rate, the total vent-gas volume increased by 0.057 L, the percent pressure rise increased by 0.89%, and the concentration of carbon dioxide decreased by 2.3%. The LFL of the gases produced from a single pouch cell during thermal runaway was $9.7\% \pm 0.7\%$. The maximum air-filled volume that becomes flammable after a thermal runaway reaction was 9.7 ± 1.6 L.

Table 10. Significant parameters of various lithium batteries

	4.5Wh 100%SOC CR123A Primary Cell Overheat without Holder	9.25Wh 30%SOC Pouch	9.62Wh 30%SOC 18650 Standard	9.62Wh 30%SOC 18650 Violent
Carbon Dioxide, %vol	NA	41.2±2.1	17.33±2.9	34.92±2.7
Carbon Monoxide, %vol	NA	3.82±0.4	4.71±0.4	3.84±0.4
Hydrogen, %vol	NA	17.0±1.2	5.98±0.9	10.25±0.7
Total Hydrocarbon, %vol	24±1.0	NA	NA	NA
Percent Pressure Rise, %	47.2±11.0	20.6±2.7	4.88±0.5	8.00±2.5
Off Gas Volume, L	1.75±0.14	0.94±0.17	0.37±0.03	0.64±0.07
Maximum Temperature, °C	338±30	404±37	222±29	314±31
Calculated LFL, %	NA	9.7±0.7	12.0±2.0	15.1±2.1
Calculated MFA, L	NA	9.7±1.61L	3.1±0.8	4.2±1.0

7. REFERENCES

- Coward, H. F., & Jones, G. W. (1952). *Limits of flammability of gases and vapors*. BM-BULL-503, Bureau of Mines, Washington, DC.
- FAA. (2016). *Lithium Battery Thermal Runaway Vent Gas Analysis*. DOT/FAA/TC-15/59, Federal Aviation Administration.
- FAA. (2020, January 1). *Events with Smoke, Fire, Extreme Heat or Explosion Involving Lithium Batteries*. Retrieved from https://www.faa.gov/hazmat/resources/lithium_batteries/media/Battery_incident_chart.pdf
- Karp, M. E. (2016). *Flammability limits of lithium-ion battery thermal runaway vent gas in air and the inerting effects of Halon 1301*. Thesis, Publication Number ATT 10291990, Rutgers The State University of New Jersey.
- Montgomery, D. C. (2013). *Design and analysis of experiments*. Hoboken, NJ: John Wiley & Sons, Inc.